REPORT DOCUMENTATION PAGE

AFRL-SR-BL-TR-02-

0073

1. REPORT DATE (DD-MM-YYYY)	2. REPORT TYPE	3. DATES COVERED (From - To)
1 January 2002	Annual Technical Report	1 Feb. 2001 - 31 Oct. 2001

4. TITLE AND SUBTITLE
Advanced Stimulated Scattering Measurements in Supercritical Fluids

5a. CONTRACT NUMBER
F49620-01-C-0020

5b. GRANT NUMBER

5c. PROGRAM ELEMENT NUMBER
61102F

6. AUTHOR(S)
Gregory W. Faris

5d. PROJECT NUMBER
2308

5e. TASK NUMBER
BX

5f. WORK UNIT NUMBER

7. PERFORMING ORGANIZATION NAME(S) AND ADDRESS(ES)
SRI International
333 Ravenswood Avenue
Menlo Park, CA 94025-3493

8. PERFORMING ORGANIZATION REPORT NUMBER

9. SPONSORING / MONITORING AGENCY NAME(S) AND ADDRESS(ES)
AFOSR/NA
801 North Randolph Street
Room 732
Arlington, VA 22203-1977

10. SPONSOR/MONITOR'S ACRONYM(S)

11. SPONSOR/MONITOR'S REPORT NUMBER(S)

12. DISTRIBUTION / AVAILABILITY STATEMENT
Approved for public release; distribution is unlimited

13. SUPPLEMENTARY NOTES

14. ABSTRACT
Stimulated Brillouin and Rayleigh scattering was applied to measurements of supercritical fluids. Measurements were performed using an injection-locked Nd:YAG laser as a pump laser and an external cavity diode laser as a probe laser. Improvements were made in stability of the probe laser, allowing more reliable operation and in the stability of the pump laser, allowing narrower bandwidth operation. Improvements were made to a supercritical cell to allow measurements in the near critical region. Software was written to enable automated analysis of measured spectra to extract the widths, shifts, and heights of the electrostrictive Brillouin, thermal Brillouin, and thermal Rayleigh peaks. Comparison of these features with theory has showed consistency of the theory through the relationships between the heights and widths of the thermal Brillouin and thermal Rayleigh peaks. Elastic and thermal properties extracted from the measurements agree with literature values for room temperature and atmospheric pressure conditions. Brillouin and Rayleigh measurements were performed over a wide range of supercritical and near-critical conditions. Interesting, unexpected structure in the behavior of the Brillouin shifts, width, and heights was observed in the supercritical region.

15. SUBJECT TERMS
Supercritical fluids, stimulated scattering, Brillouin scattering, Rayleigh scattering, elastic properties, thermal properties

16. SECURITY CLASSIFICATION OF:			17. LIMITATION OF ABSTRACT	18. NUMBER OF PAGES	19a. NAME OF RESPONSIBLE PERSON
a. REPORT	b. ABSTRACT	c. THIS PAGE			Julian M. Tishkoff
Unclassified	Unclassified	Unclassified	UL	43	19b. TELEPHONE NUMBER (include area code) (703) 696-8478

Standard Form 298 (Rev. 8-98)
Prescribed by ANSI Std. Z39.18

SRI International

Final Report • January 2002

ADVANCED STIMULATED SCATTERING MEASUREMENTS IN SUPERCRITICAL FLUIDS

Prepared by:

Gregory W. Faris
Molecular Physics Laboratory

SRI Project 11222

Contract Number F49620-01-C-0020

MP 02-003

Prepared for:

Air Force Office of Scientific Research
AFOSR/NA
801 North Randolph Road, Room 732
Arlington VA 22203-1977

Attn: Dr. Julian Tishkoff

333 Ravenswood Avenue • Menlo Park, CA 94025-3493 • (650) 326-6200

TABLE OF CONTENTS

OBJECTIVES

The objectives of this research are to develop stimulated scattering as a diagnostic for supercritical fluids, and use this technique to improve our understanding of fluids in the supercritical state.

The study of supercritical fluids and flows requires new diagnostic techniques. Currently available techniques such as laser-induced fluorescence (LIF) and coherent anti-Stokes Raman scattering (CARS) are complicated by increased molecular interactions, leading to stronger quenching, larger absorption and refractive index, and incomplete understanding of the influence of local conditions on spectroscopic parameters such as linewidths, nonresonant background contributions, and quenching rates. We believe that stimulated scattering techniques hold great promise for studying supercritical fluids.

STATUS OF EFFORT

Stimulated Brillouin and Rayleigh scattering was applied to measurements of supercritical fluids. Measurements were performed using an injection-locked Nd:YAG laser as a pump laser and an external cavity diode laser as a probe laser. Improvements were made in stability of the probe laser, allowing more reliable operation and in the stability of the pump laser, allowing narrower bandwidth operation. Improvements were made to a supercritical cell to allow measurements in the near critical region. Software was written to enable automated analysis of measured spectra to extract the widths, shifts, and heights of the electrostrictive Brillouin, thermal Brillouin, and thermal Rayleigh peaks. Comparison of these features with theory has showed consistency of the theory through the relationships between the heights and widths of the thermal Brillouin and thermal Rayleigh peaks. Elastic and thermal properties extracted from the measurements agree with literature values for room temperature and atmospheric pressure conditions. Brillouin and Rayleigh measurements were performed over a wide range of supercritical and near-critical conditions. Interesting, unexpected structure in the behavior of the Brillouin shifts, width, and heights was observed in the supercritical region.

INTRODUCTION

Supercritical fuels and mixing are becoming very important for Air Force projects such as advanced air breathing propulsion systems and advanced launch boosters. The relative lack of experience with and understanding of the fluid properties, fluid dynamics and mixing, and chemical kinetics under such conditions requires the development and application of diagnostic techniques that are well suited to characterize the new features and processes that may occur. These techniques are especially important because diagnostic approaches for low pressures cannot be easily adapted to supercritical conditions. This research on stimulated scattering is very well suited to performing diagnostics on supercritical fluids.

Supercritical conditions are important in two significant areas. For air breathing propulsion, increasing demands are being placed on fuel as a coolant for the engine, environmental control systems, electronics, and at high Mach numbers, even the airframe. These cooling needs will heat the fuel into the supercritical phase. Relatively little is known about the properties of fuels in the supercritical regime or the effects of injecting supercritical fuel into subcritical turbines or ramjets. Diagnostics are required to understand the state and properties of the fuel as it is heated and to help understand the effect of these supercritical fuels on engine performance.

For high pressure rocket propulsion, fuel or oxidant may transform from a subcritical to a supercritical state during injection into the combustion chamber. For example, in liquid oxygen-hydrogen rockets, liquid oxygen is injected at supercritical pressure and subcritical temperature and is heated to supercritical temperature in the combustion chamber. Improved diagnostics are required to study the significance of this transcritical mixing on rocket engine performance.

High temperatures create many unusual problems for fuel systems. Thermal cracking changes fuel properties and can produce gums and solids that freeze valves and foul fuel nozzles and heat exchangers. In the supercritical regime, fuels have liquid-like densities and gas-like diffusivities and viscosities. The changing heat load during the flight of advanced aircraft will lead to widely varying fuel properties during a mission; fuel systems must perform well under all these conditions. In the region of the critical point, destructive flow and pressure instabilities can arise. These various effects demand thorough investigation of proposed fuels and fuel systems under anticipated conditions.

We performed research into new diagnostic techniques that can aid the design and diagnostic evaluation of new supercritical fuel systems for next generation Air Force propulsion systems. These techniques may be used for obtaining a better understanding of supercritical fuels behavior and mixing and for evaluating fuel delivery systems and supercritical fuel mixing. This information is critical in ensuring reliable performance of next generation aircraft.

OPTICAL DIAGNOSTICS FOR SUPERCRITICAL FLUIDS

Traditional optical diagnostic techniques can be broadly grouped into two classes: (1) *hydrodynamic* diagnostics, including schlieren, interferometry, and tracer particles, and (2) *molecular* diagnostics, including laser-induced fluorescence (LIF) and coherent anti-Stokes Raman scattering (CARS). Techniques from these two classes will continue to be important in characterizing supercritical mixing and combustion. Hydrodynamic diagnostics will be useful for determining qualitative behavior, gross structure, and mapping of flow fields. Indeed, this type of diagnostic has been used for several studies of supercritical mixing.[1-4]

Molecular diagnostics provide a fine-scale picture of the details of molecular interactions, radical concentrations, local temperature, and velocities. Quantitative interpretation of molecular diagnostics remains a relative weakness, especially in the supercritical regime. Extending techniques such as LIF and CARS to high pressure, multiphase environments is complicated by increased molecular interactions, leading to stronger quenching, larger absorption and refractive index, broader linewidths, and incomplete understanding of the influence of local conditions on spectroscopic parameters such as linewidths, nonresonant background contributions, and quenching rates.

Our research involves a third class of diagnostics techniques that can effectively investigate the unusual conditions expected in supercritical fluids. These diagnostics are based on stimulated Rayleigh, Brillouin, and Raman scattering measurements. We call this class *collective* diagnostics, because they involve collective material motions. These material motions are in turn fundamentally linked to useful and significant underlying physical parameters.

Near the critical point, the gaseous and liquid forms of a fluid become indistinguishable. Such a fluid has unusual properties, such as liquid-like densities and gas-like diffusivities and viscosities, with negligible surface tension, no heat of vaporization, infinite isothermal compressibility, and enhanced chemical reactivity. The large compressibility and thermodynamic equivalence of the liquid and gaseous forms at the same pressure mean that a near-critical fluid is continually condensing and evaporating, which really mean aggregating and dissociating, because there is no actual separation of phases.

This brief description illustrates that near critical and supercritical fluids will experience a range of collective effects that may greatly influence the mechanisms of mixing and combustion. For example, the concept of a droplet is no longer well defined, yet the formation and breakup of droplets remain important to understanding both how a "liquid-like" fuel mixes with a "gas-like" oxidizer and how chemical reactions are modified. The spatial scale of these collective effects should be about 1-1000 μm, much larger than molecules, and difficult to visualize and quantify with path-integrated measurements such as schlieren or interferometry. Thus there is a need for new diagnostic techniques, which is filled by stimulated scattering techniques.

STIMULATED SCATTERING

Rayleigh, Brillouin, and Raman scattering occur commonly as spontaneous scattering. These scattering processes arise from natural oscillation modes of materials and can be used to determine the physical parameters responsible for those oscillations. When these collective modes are excited with a powerful laser, the mode oscillations can be driven so hard that they grow exponentially. This phenomenon is called stimulated scattering. The dominant advantage of stimulated scattering is that the scattered signal can be made arbitrarily large; otherwise, these processes produce extremely weak signals. By using a probe to measure the induced amplification, we can obtain very good quantitative results. This technique is distinct from the stimulated scattering that builds up from noise, in which case quantification is very difficult.

The large signals from stimulated scattering are particularly helpful for investigating Rayleigh and Brillouin scattering, where the weak signals available from spontaneous scattering are difficult to discriminate from background excitation light. Other advantages of stimulated scattering include excellent temporal resolution, and improved spectral resolution and signal-to-noise ratio. Furthermore, the use of two laser beams allows spatial registration and point measurement of local conditions.

With a single detection system, all three processes—Rayleigh, Brillouin, and Raman—can be measured. These processes together provide measurements of a wide range of material properties. Rayleigh scattering provides information on thermal properties, compositional fluctuations, and density; Brillouin scattering on compressional or elastic properties and density; and Raman scattering on chemical and compositional properties, density, and temperature. While spontaneous Brillouin[5] and Raman[4,6,7] scattering have been applied to supercritical fluids, the use of stimulated scattering for supercritical fluids is new.

The basic arrangement for stimulated scattering measurements is shown in Figure 1. The pump laser sets up an electric polarization oscillating at the characteristic frequency of a scattering mode of the material.[8] For a strong input laser pulse, this polarization acts as a driving force, leading to amplification of both the material oscillation and a scattered optical wave. The optical amplification is detected as a gain or loss on the probe beam. Spatial resolution is determined by the overlap volume of the pump and probe beams.

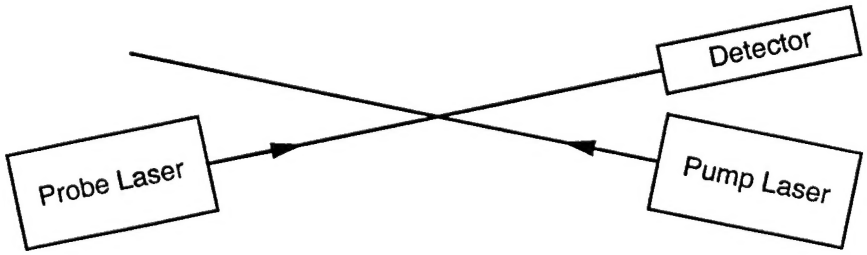

Figure 1. Basic experimental arrangement for stimulated scattering measurements.

When using spontaneous scattering, it can be quite difficult to discriminate the Rayleigh and Brillouin scattered signals against the background excitation light, even under ideal detection conditions. However, the large signals from stimulated scattering processes result in no problems in discriminating against background light. This can be seen in Figures 5-9 in the Accomplishments / New Findings section. Even though these measurements are performed within a few GHz (a fraction of 1 cm^{-1}) of the wavelength of the pulsed excitation laser, there is no contribution of scattered background light to the measurement.

Other advantages of stimulated scattering over spontaneous scattering include exceptional temporal resolution, improved spectral resolution (limited by the laser linewidths rather than a spectrometer or interferometer), and very high signal-to-noise ratios. Furthermore, the use of two laser beams allows spatial registration and point measurement of local conditions.

Rayleigh scattering results from refractive index variations due to thermal waves or diffusive density fluctuations and compositional fluctuations. Brillouin scattering results from refractive index variations due to sound waves or traveling density or pressure fluctuations.

In a single-component fluid, the positions, strengths, line shapes, and linewidths in the combined Rayleigh and Brillouin scattering spectrum provide information about the temperature, density, isothermal compressibility χ_T, the heat capacity ratio c_P/c_V, the thermal diffusivity D_T, the acoustic attenuation coefficient Γ, the adiabatic sound velocity c_S, and the longitudinal kinematic viscosity or effective mass diffusion coefficient D_V.[9] Values of these parameters obtained from stimulated scattering in hexane are given in Table 1 of the Accomplishments / New Findings section. An additional oscillatory mode[10,11] provides information on the exchange of energy between the internal vibrational modes and translational modes. Near the critical point, several of these parameters approach exceptional values, e.g., $c_S \rightarrow 0$ and $\chi_T \rightarrow \infty$. Critical opalescence is an extreme case of scattering off density fluctuations. One of the first practical uses of spontaneous Brillouin scattering in gases was the investigation of the speed of sound near the critical point.[5]

In two-component fluids, additional information can be obtained from Rayleigh and Brillouin scattering measurements.[12] Even in a nominally well-mixed sample, fluctuations will exist in relative concentration or mole fraction. These fluctuations contribute to scattering that appears as part of the central Rayleigh line, with a linewidth depending on the binary diffusion coefficients D_{ij}. In addition, the differences in molecular weight between the two components means that there are actually three speeds of sound in a binary mixture: the hydrodynamic or adiabatic speed of sound of the mixture, $c_S \sim [kT/(m_1\chi_1 + m_2\chi_2)]^{1/2}$, and the speeds of sound of the individual components, $\sim [kT/m_1]^{1/2}$ and $\sim [kT/m_2]^{1/2}$. Acoustic waves traveling at the component speeds are rapidly damped, but show up as well-defined features at characteristic frequencies in the Brillouin spectrum of the mixture. The linewidths of these features could be used to determine the binary viscosity coefficients, η_{ij}. In principle, such Brillouin scattering measurements in mixtures could be used to determine both the local chemical composition and the rate of chemical mixing.

Raman scattering from molecules is a well established technique in combustion diagnostics. Spontaneous Raman scattering is one of the few optical diagnostic techniques that has been used to date on supercritical fluids.[4,6,7,13] Stimulated Raman scattering can be performed with essentially the same apparatus as the stimulated Rayleigh and Brillouin measurements and provides stronger signals, higher spectral resolution, and better signal-to-noise ratios than spontaneous Raman scattering. Information provided by stimulated Raman scattering includes chemical composition, density, and temperature. Interpretation of stimulated Raman scattering measurements is simpler than for CARS, because the signal is directly proportional to the imaginary part of the third-order nonlinear susceptibility (or to the Raman scattering cross section) rather than to the squared magnitude of the sum of real and imaginary parts of the third-order susceptibility, as is the case for CARS.[14]

The stimulated scattering techniques are widely applicable. Besides liquids and supercritical fluids, we have used stimulated Brillouin and Rayleigh scattering to perform measurements in glasses, crystals, and gases[8,14,15] without the requirement of detailed spectroscopic information on these materials. Our supercritical experiments are aided by long term research at SRI on supercritical fluids, including studies of supercritical water oxidation[16] and supercritical fluid extraction.[17]

The laser requirements for our stimulated Rayleigh and Brillouin measurements are quite modest. The pump beam energy is only ~ 40 μJ, and the probe beam is provided by a diode laser. Thus, stimulated scattering could be used even as an on board monitor of fuel state and properties.

Parameters currently of interest to the Air Force for supercritical fuels include compressibility, sonic velocity, density and phase, and chemical composition.[18] All these parameters can be provided directly by stimulated scattering measurements. Thus stimulated scattering will play a very important role in understanding fuel performance and in diagnosing fuel system performance, critical steps in assuring the performance of next generation aircraft. We are one of only a handful of groups that have performed stimulated Rayleigh and Brillouin experiments, and we are the only group applying these techniques to supercritical fluids.

ACCOMPLISHMENTS / NEW FINDINGS

We are using stimulated scattering (stimulated Rayleigh, Brillouin, and Raman scattering) to study supercritical fluids. New diagnostics are needed in the supercritical regime because low pressure diagnostics do not work well. From our measurements we can determine thermal, compressional, and compositional properties of supercritical fuels *in situ*. These techniques should improve our knowledge of fluid properties in the supercritical state.

EXPERIMENT

Stimulated scattering allows measurements of the physical properties of fuels, including compressibility, speed of sound, thermal diffusivity, and chemical composition, density, and temperature while at supercritical conditions. This is significant, because much work on supercritical fuels has been performed after returning the fuels to ambient conditions, rather than in the supercritical state. Our work complements well work on optical diagnostics of supercritical fuels being performed at Wright-Patterson using spontaneous Raman and fluorescence measurements.

The optical arrangement for stimulated Rayleigh / Brillouin scattering is shown in Figure 2. The pump laser is an injection-seeded Nd:YAG laser. By lowering the oscillator pump energy, we obtain a transform-limited linewidth of about 10 MHz. The probe laser is an external cavity diode laser. The two lasers are overlapped in the cell in a counter-propagating geometry. To reduce scattered light, the measurement cell is tilted slightly and the probe light is spatially filtered through an optical fiber. The probe laser wavelength is measured using a Fizeau wavemeter. Because of the narrow linewidths of the Rayleigh peak, transient effects are important. We avoid transient effects by using the time-integrated gain signal.[8,19]

Improvements were made to both the pump and probe lasers. A new seed laser was installed on the pump laser to improve the power available for injection locking the pump laser. This allowed operation at longer pulsewidths, which corresponds to a narrower linewidth for the Fourier transform limited laser, and better spectral resolution in the measurements. The probe laser cavity was optimized through fine adjustment of the cavity length to allow more reliable single mode tuning. This optimization reduced the number of spectra that were unusable due to laser mode hops or laser instability.

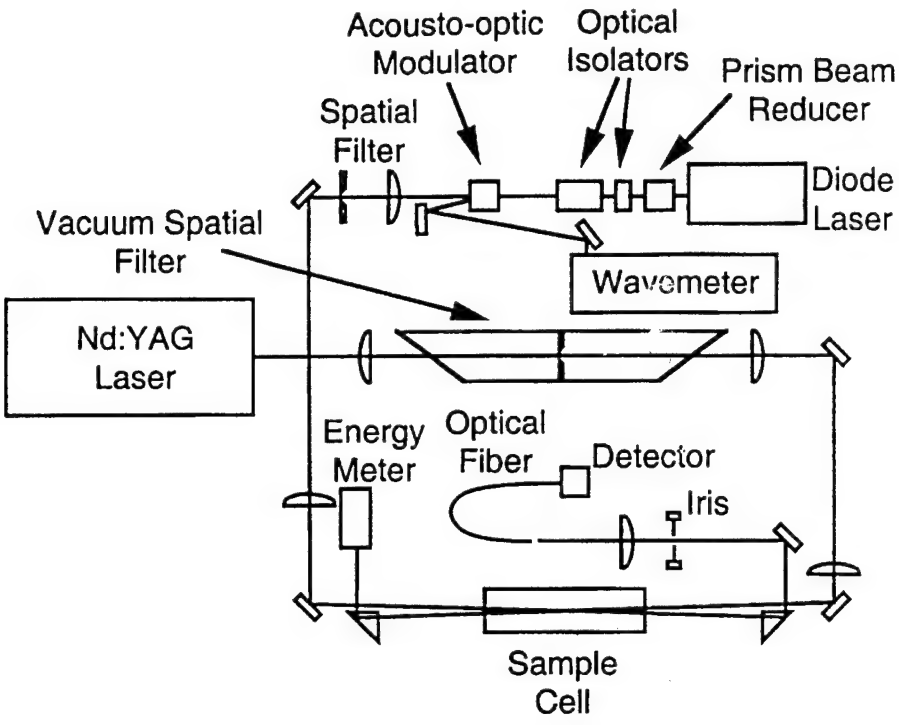

Figure 2. Apparatus for stimulated Brillouin and stimulated Rayleigh scattering at 1064 nm.

We have previously reported the design and construction of a cell for capable of operation up to 600 K and 2000 psi. During design of that cell, we have drawn on information gained from conversations with Tim Edwards and Chris Bunker of AFRL–Wright-Patterson in their work on high pressure / high temperature systems. We have subsequently made a number of modifications to this cell. To avoid leaks at high temperatures, we substituted titanium bolts for the steel bolts, and glass windows for the fused silica windows. Titanium and glass have nearly the same thermal expansion coefficient. When operating the cell at high temperature, we found that convection near the windows caused beam wander, particularly in the region of the critical point. To minimize these effects, we have shortened the cell to an internal length of 2.5 cm. A schematic of this short cell is shown in Figure 3. The cell comprises two windows separated by an internal length of 2.5 cm. The windows are sealed using graphite seals. A schematic of the overall high pressure system is shown in Figure 4. The ends of the heater surrounding the cell were sealed using ceramic caps with windows in them. To allow measurements in the region of the critical point and above, we carefully sealed all openings in these end caps to minimize convection currents.

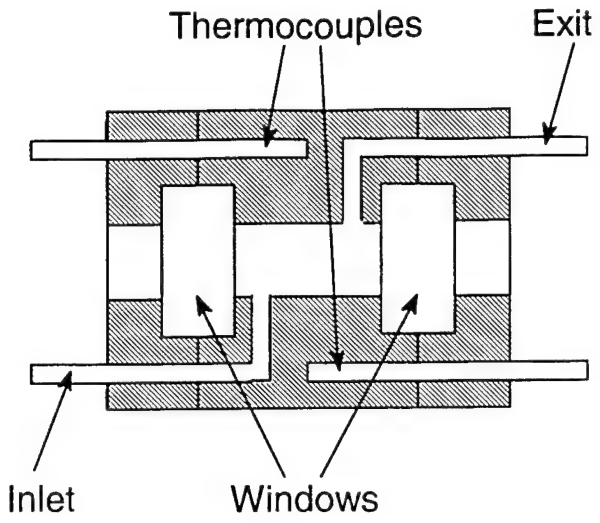

Figure 3. Schematic diagram of the supercritical cell.

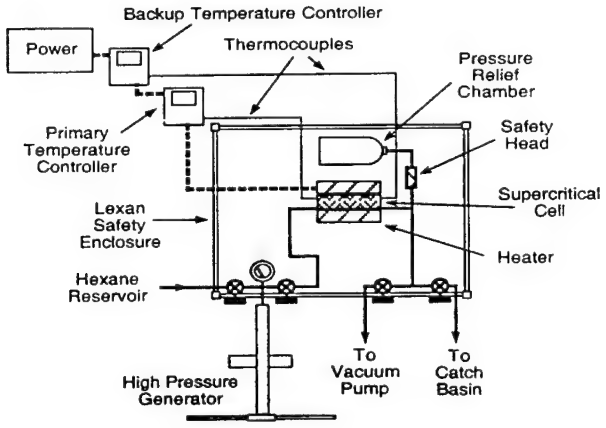

Figure 4. Overall high pressure system.

We have used the modified cell to perform stimulated scattering measurements in the supercritical and near critical regimes. These are the first stimulated Rayleigh and stimulated Brillouin scattering at supercritical conditions to our knowledge. An example of measurements performed at 200 C and 630 psi is shown in Figure 5. The abscissa is the difference in frequency between the pump and probe lasers determined by the wavemeter. The gain signal is divided by the pump and probe laser intensities to compensate for intensity fluctuations in each laser. The outer two peaks are Brillouin peaks; the central pair of peaks is due to stimulated Rayleigh

scattering. The positive-going Brillouin peak to the left is a gain peak, corresponding to transfer of power from the Nd:YAG laser to the probe laser. The negative-going peak to the right is a loss peak, wherein power is transferred from the probe laser to the pump laser.

We developed software to enable automated analysis of measured spectra to extract the widths, shifts, and heights of the electrostrictive Brillouin, thermal Brillouin, and thermal Rayleigh peaks. Macros were written to operate in the Igor graphics environment to iterate through a list of spectra and perform fits to all the peaks without manual intervention. Appropriate lineshapes are used for each spectral feature. The electrostrictive Brillouin lineshape is described by the real part of the complex Lorentzian profile; the thermal Brillouin and Rayleigh lineshapes are described by the imaginary parts of a complex Lorentzian profile.[20] The measured lineshapes are given by the convolution of the Gaussian spectral lineshape of the Nd:YAG pump laser with these Lorentzian profiles. These convolved lineshapes may be expressed as the real and imaginary parts of the complex error function for the Brillouin and Rayleigh peaks, respectively (the former is a Voigt profile). Complex error function fits to the data were performed using the algorithm of Humlicek,[21,22] and the Igor graphics program (WaveMetrics, Inc.). We used the Fourier-transform limited linewidth calculated from pulsewidth as the spectral linewidth of the pump laser. To eliminate the contribution of the 10 Hz dither used to lock the Nd:YAG laser to the seed laser, measurements were performed at 5 Hz. The seed laser linewidth is specified to be less than 300 kHz in 50 ms.

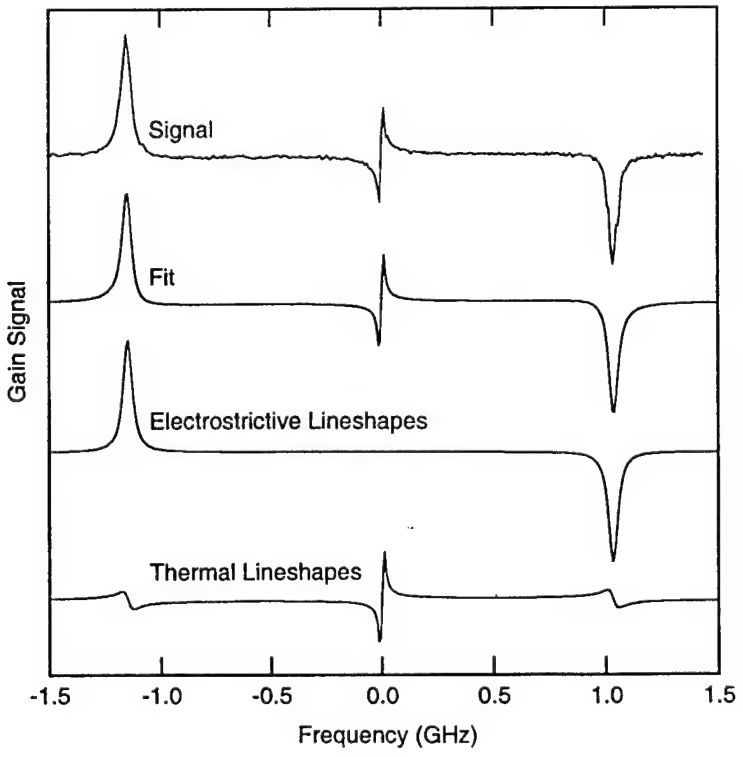

Figure 5. Stimulated Rayleigh and Brillouin spectrum for hexane at 200°C and 630 psi.

The full fit to the Rayleigh/Brillouin spectrum is shown as the curve labeled "fit" in Figure 5. Very good agreement is found between the measured and fit lineshapes (see also Figures 6 and 7). The electrostrictive and thermal contributions to the overall fit are shown separately at the bottom of Figure 5. The thermal scattering is due to absorption by OH or CH overtone or combination bands. This absorption increases the size of the stimulated Rayleigh peak (it is otherwise difficult to observe) and causes an asymmetry in the stimulated Brillouin peak due to the imaginary Lorentzian shape of the thermal Brillouin scattering.

Expanded spectra for stimulated Brillouin and stimulated Rayleigh scattering in hexane at room temperature are shown in Figures 6 and 7. Also shown are fits to these spectra. The frequency values for the stimulated Rayleigh peak in Figure 7 were determined from the heterodyne signal between the seed and probe lasers. This peak is quite narrow. The average linewidth determined from multiple fits such as shown in Figure 7 gives value of 7.9±3.2 MHz, which is in good agreement with the value expected from the thermal diffusivity for n-hexane. These measurements were performed with a pulsewidth for the Nd:YAG laser of approximately 30 ns, which corresponds to a full width half maximum spectral linewidth of about 15 MHz. Thus the laser linewidth is about twice the measured linewidth of the Rayleigh peak. The good agreement with the expected linewidth confirms that the Nd:YAG laser has a transform-limited linewidth of 15 MHz. The spectroscopic and thermodynamic properties for n-hexane determined from numerous such fits are given in Table 1. The errors are standard deviations of values averaged from 14 or more measurements. These calculations use the refractive index for hexane (extrapolated to 1064 nm from a literature expression[23]) as appropriate.[20] Good agreement is obtained with values available in the literature.

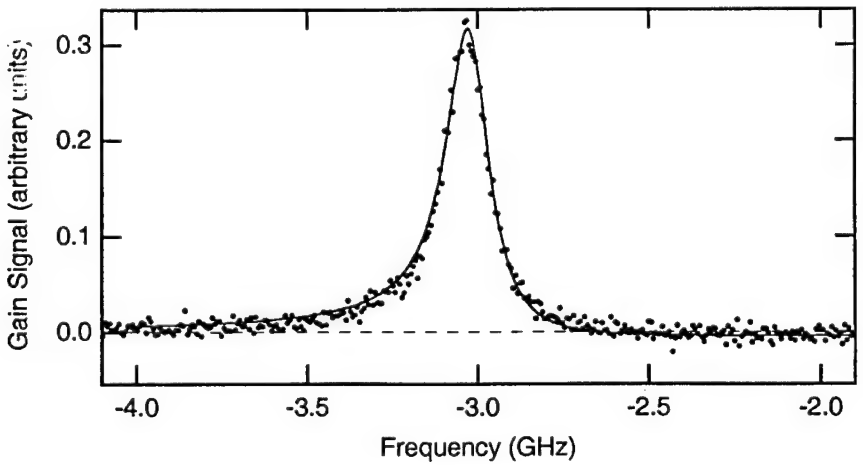

Figure 6. Data (points) and fit (solid line) for stimulated Brillouin gain peak for n-hexane at 1064 nm. Stimulated thermal Brillouin scattering gives an asymmetry to the peak.

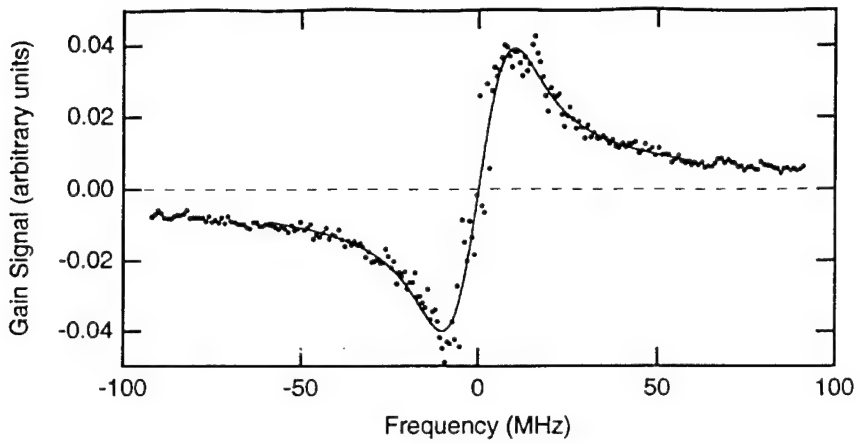

Figure 7. Data (points) and fit (solid line) for stimulated thermal Rayleigh scattering in n-hexane at 1064 nm.

Table 1. Properties measured in hexane using stimulated Rayleigh /Brillouin scattering at 1064 nm.

Property	Our Results	Literature Values
Brillouin shift	2.91±0.06 GHz	
Brillouin width	151±8 MHz	
Rayleigh width	7.9±3.2 MHz	
Ratio of electric to absorptive coupling constants	8.8±0.6	
Acoustic damping time	1.06 ns	
Acoustic velocity	1.14 km/s	1.10 km/s
Acoustic attenuation coefficient	8.3×10^5 m^{-1}	7.4×10^5 m^{-1}
Effective mass diffusion coefficient	7.4×10^{-6} m^2/s	
Isentropic compressibility	1.2×10^{-9} m^2/N	
Thermal diffusivity	9.6×10^{-8} m^2/s	9.2×10^{-8} m^2/s

We have observed electrostrictive stimulated Rayleigh scattering in a liquid and created a transition to stimulated thermal Rayleigh scattering with the addition of an absorbing liquid. With the proper amount of absorption, the electrostrictive and thermal contributions to the scattering exactly cancel, resulting in no stimulated Rayleigh scattering. This effect is shown in Figure 8. The top curve shows a pure electrostrictive stimulated Rayleigh peak in pure freon 113. With an addition of 0.1% ethanol (an absorption coefficient of 0.00012 cm^{-1}) the stimulated thermal scattering cancels the stimulated electrostrictive scattering (center curve). With addition of more ethanol, the stimulated peak has flipped over (bottom curve)

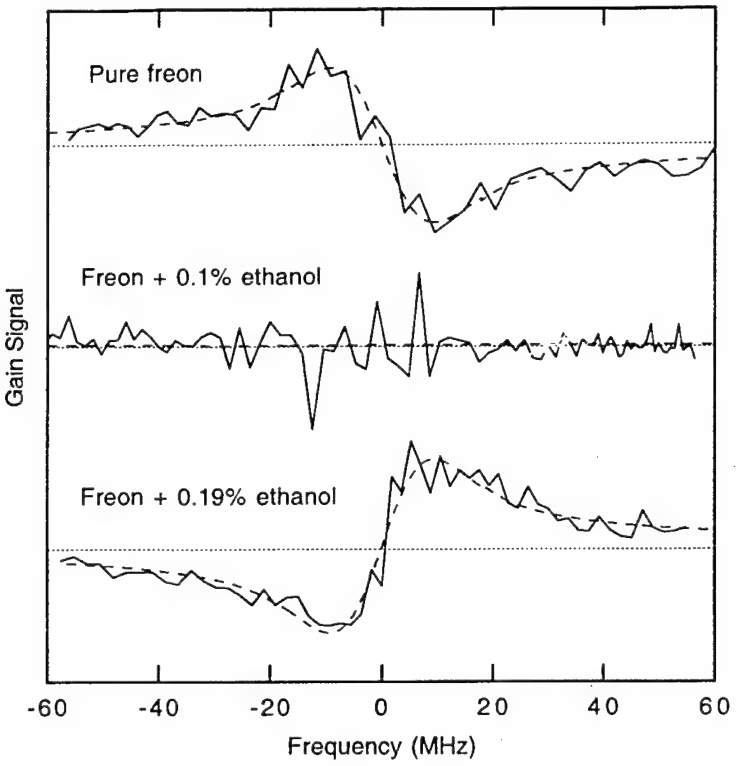

Figure 8. Measured stimulated Rayleigh gain signal (solid curve) and fitted profile (dashed curve) in pure freon 113 (top), and freon with 0.1% ethanol (middle) and 0.19% ethanol (bottom).

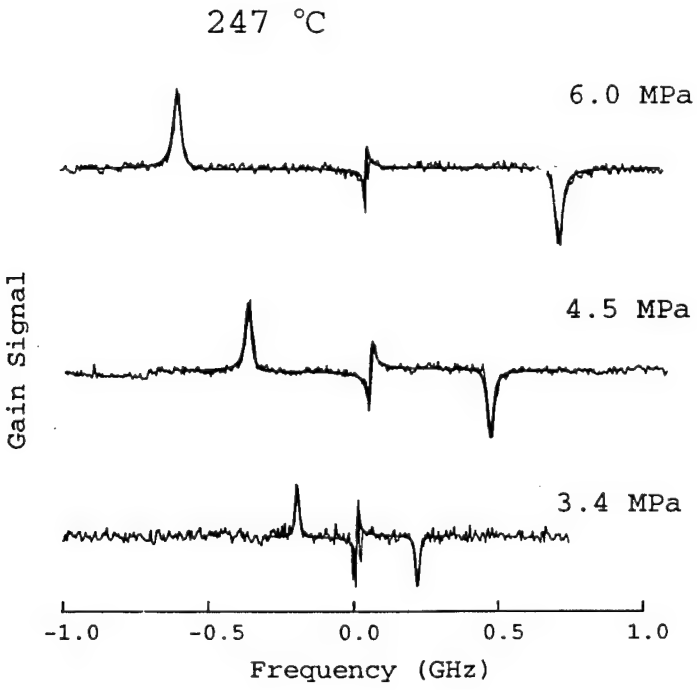

Figure 9. Stimulated Rayleigh / Brillouin scattering spectrum for n-hexane measured at 1064 nm near the critical temperature for three different pressures. The spectral fits to the data including the electrostrictive and thermal components to the fit are shown.

Examples of stimulated Rayleigh / Brillouin scattering spectra measured in n-hexane near the critical temperature at three different pressures are shown in Figure 9. The peaks to the left and right of each spectrum are the gain and loss Brillouin peaks, respectively. The central peak is the stimulated Rayleigh peak. Optical absorption has increased the size of the Rayleigh peak and produced asymmetry to the Brillouin peaks. Also shown in Figure 9 are fits to the data (thicker lines). These fits include the appropriate lineshapes for each peak and the laser spectral width. Fits of this type enable calculation of material properties.

We have investigated fluctuations near the critical point. These fluctuations can cause flow and pressure instabilities, which have been found to have destructive effects on tubing.[24,25] Avoiding these fluctuations is very important for fuel systems that transition into the supercritical regime. The critical point for n-hexane occurs at a pressure 31 kPa and temperature of 234 ° C. Figures 10-14 present stimulated Brillouin scattering properties for n-hexane at 1064 nm at sub-, near-, and supercritical conditions. The striking feature in all the figures presented is the discontinuity in the observed properties that occurs at the critical point.

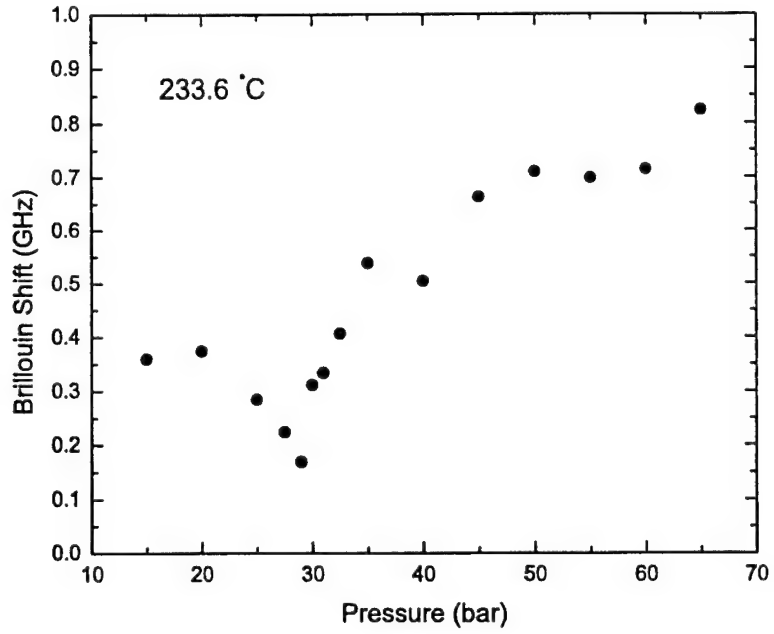

Figure 10. The Brillouin shift observed in stimulated Brillouin scattering for n-hexane at 1064 nm near the critical temperature as a function of pressure. The Brillouin shift has a minimum in the region of the critical point.

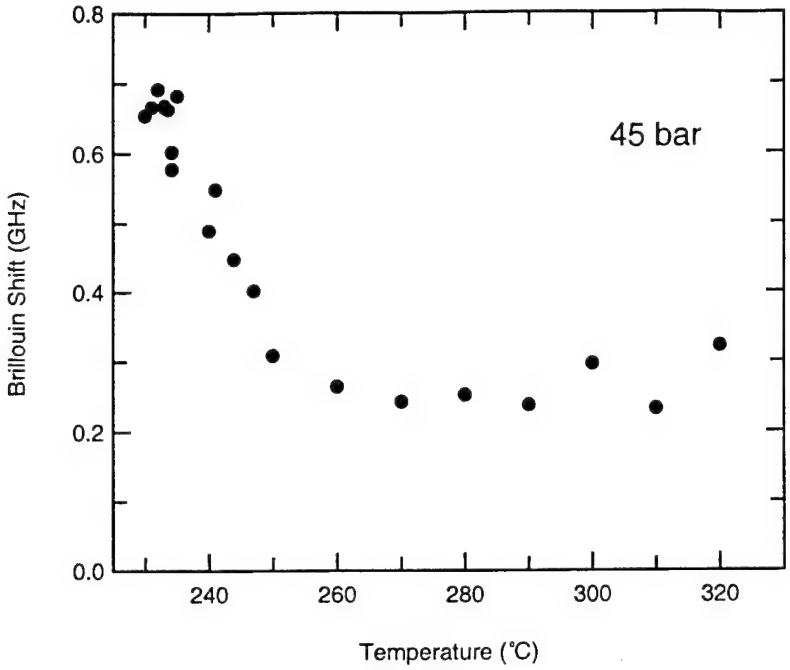

Figure 11. The Brillouin shift observed in stimulated Brillouin scattering for n-hexane at 1064 nm for a pressure of 45 bar as a function of temperature. A local maximum is observed near the critical point.

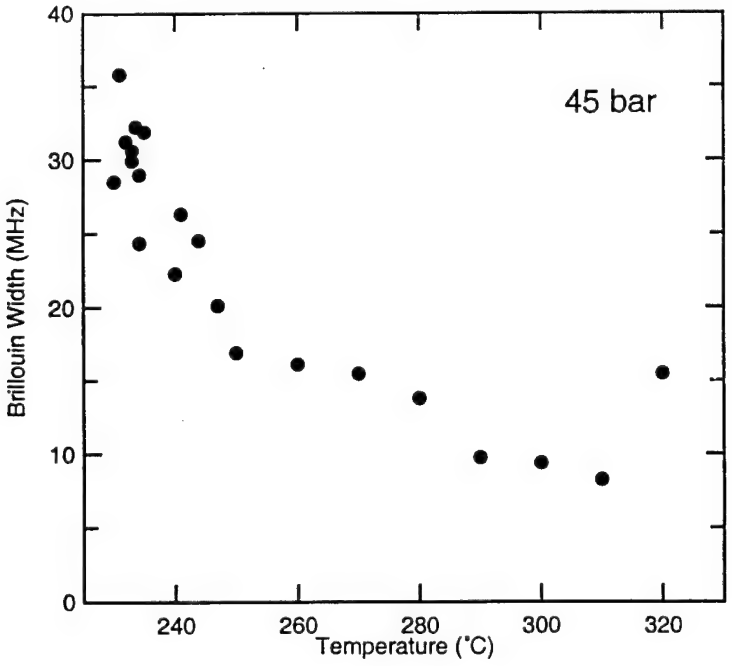

Figure 12. The peak width observed in stimulated Brillouin scattering for n-hexane at 1064 nm for a pressure of 45 bar as a function of temperature.

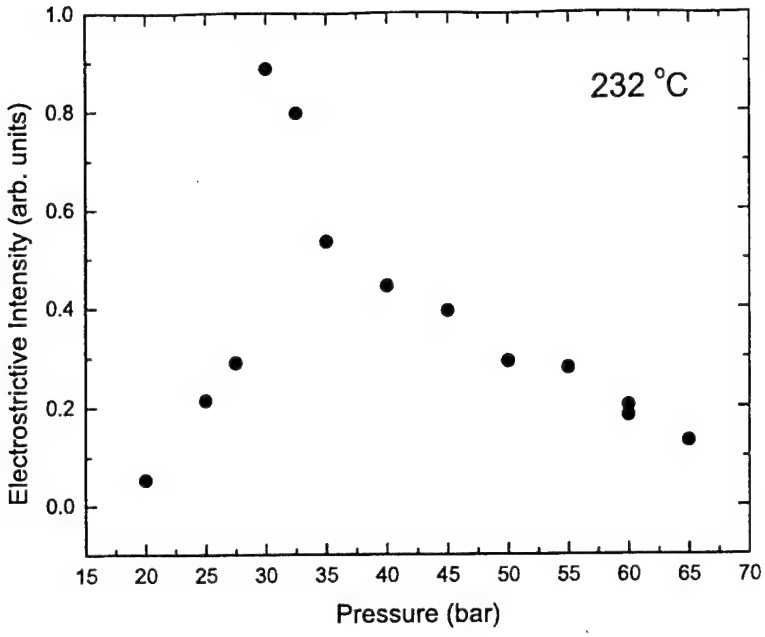

Figure 13. The intensity of the electrostrictive component of stimulated Brillouin scattering for n-hexane at 1064 nm for a temperature of 232 ° C as a function of pressure. A sharp increase in intensity is observed near the critical point.

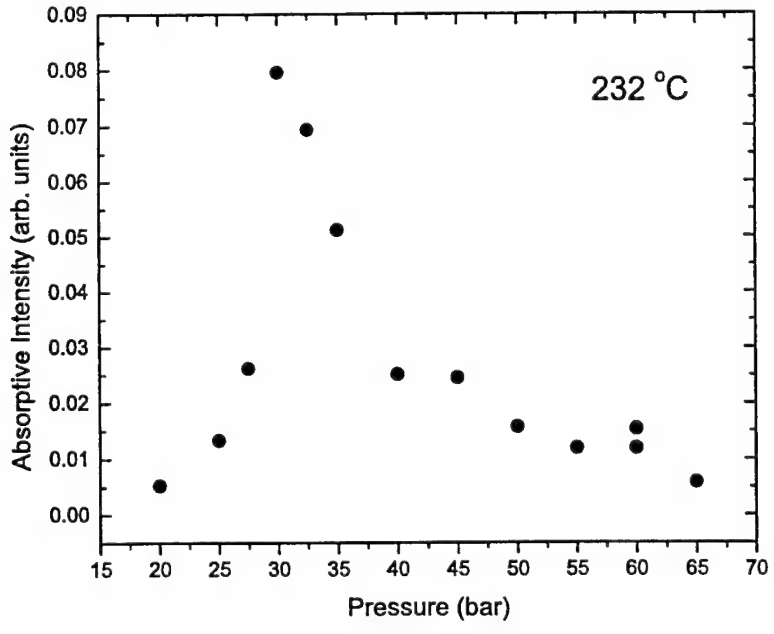

Figure 14. The intensity of the absorptive component of stimulated Brillouin scattering for n-hexane at 1064 nm for a temperature of 232 ° C as a function of pressure.

REFERENCES

1. J. A. Newman and T. A. Brzustowski, "Behavior of a liquid jet near the thermodynamic critical region," AIAA J. **9**, 1595-1602 (1971). (from citation)

2. R. D. Woodward, D. G. Talley, T. J Anderson, and M. Winter, "Shadowgraphy of transcritical cryogenic fluids," presented at 6th Annual Penn State PERC Symposium, NASA Lewis Research Center, Cleveland, OH, 1994.

3. W. Mayer and H. Tamura, "Flow visualization of supercritical propellant injection in a firing LOX/GH2 rocket engine," presented at 31st AIAA/ASME/SAE/ASEE Joint Propulsion Conference & Exhibit, San Diego, CA, 1995.

4. R. D. Woodward and D. G. Talley, "AIAA 96-0468, Raman imaging of transcritical cryogenic propellants," presented at 34th Aerospace Sciences Meeting & Exhibit, Reno, NV, 1996.

5. R. W. Gammon, H. L. Swinney, and H. Z. Cummins, "Brillouin scattering in carbon dioxide in the critical region," Phys. Rev. Lett. **19**, 1467-1469 (1967).

6. M. S. Brown and R. R. Steeper, "CO_2-based thermometry of supercritical water oxidation," Appl. Spectrosc. **45**, 1733-1738 (1991).

7. W. Kohl, H. A. Lindner, and E. U. Franck, "Raman spectra of water to 400°C and 3000 bar," Ber. Bunsenges. Phys. Chem. **95**, 1586-1593 (1991).

8. G. W. Faris, L. E. Jusinski, and A. P. Hickman, "High-resolution stimulated Brillouin gain spectroscopy in glasses and crystals," J. Opt. Soc. Am. B **10**, 587-599 (1993).

9. B. J. Berne and R. Pecora, *Dynamic Light Scattering* (John Wiley & Sons, New York, 1976).

10. R. D. Mountain, "Spectral distribution of scattered light in a simple fluid," Rev. Mod. Phys. **38**, 205-214 (1966).

11. W. S. Gornall, G. I. A. Stegeman, B. P. Stoicheff, R. H. Stolen, and V. Volterra, "Identification of a new spectral component in Brillouin scattering of liquids," Phys. Rev. Lett. **17**, 297-299 (1966).

12. R. P. C. Schram, G. H. Wegdam, and A. Bot, "Rayleigh-Brillouin light-scattering study of both fast and slow sound in binary gas mixtures," Physical Review A: Atomic, Molecular, and Optical Physics **44**, 8062-8071 (1991).

13. T. Edwards, "AIAA 93-0807, USAF supercritical hydrocarbon fuels interests," presented at 31st Aerospace Sciences Meeting & Exhibit, Reno, NV, 1993.

14. G. W. Faris, "Brillouin gain spectroscopy in glasses and crystals," in *Applied Laser Spectroscopy*, W. Demtröder and M. Inguscio, Eds. (Plenum Press, New York, 1990), pp. 307-312.

15. G. W. Faris, L. E. Jusinski, M. J. Dyer, W. K. Bischel, and A. P. Hickman, "High-resolution Brillouin gain spectroscopy in fused silica," Opt. Lett. **15**, 703-705 (1990).

16. D. S. Ross and I. Jayaweera, "Conversions of organic material in hydrothermal media," presented at Americal Chemical Society Meeting, 1994.

17. S. Ventura, G. Hum, and S. Narang, Supercritical CO_2 extraction of porous absorbants, GRI report (1992).

18. T. Edwards, personal communication (1996).

19. G. W. Faris, M. Gerken, C. Jirauschek, D. Hogan, and Y. Chen, "High-spectral-resolution stimulated Rayleigh–Brillouin scattering at 1 μm," Opt. Lett. **26**, 1894-1896 (2001).

20. W. Kaiser and M. Maier, "Stimulated Rayleigh, Brillouin, and Raman spectroscopy," in *Laser Handbook*, F. T. Arecchi and E. O. Schulz-Dubois, Eds. (North-Holland, Amsterdam, 1972), Vol. 2, pp. 1077-1150.

21. J. Humlicek, "Optimized computation of the Voigt and complex probability functions," J. Quant. Spectrosc. Radiat. Transfer **27**, 437-444 (1982).

22. F. Schreier, "The Voigt and complex error function: A comparison of computational methods," J. Quant. Spectrosc. Radiat. Transfer **48**, 743-762 (1992).

23. H. El-Kashef, "Molecular properties of hexane," J. Modern Opt. **46**, 1389-1399 (1999).

24. W. S. Hines and H. Wolf, "Pressure oscillations associated with heat transfer to hydrocarbon fluids at supercritical pressures and temperatures," ARS Journal , 361-366 (March 1962).

25. L. E. Faith, G. H. Ackerman, and H. T. Henderson, Heat sink capability of jet A fuel: Heat transfer and coking studies, NASA Report No. CR-72951 (1971).

PERSONNEL

The following personnel participated in the research supported by this contract:

Gregory W. Faris, Senior Physicist, principal investigator and lead experimentalist.

Kostas Kalogerakis, Research Chemical Physicist, experimentalist.

Rachel Forman, Undergraduate Student, experimentalist.

Benjamin Blehm, Undergraduate Student, experimentalist.

PUBLICATIONS

The following publications were made on research supported by this contract:

G. W. Faris, M. Gerken, C. Jirauschek, D. Hogan, and Y. Chen, "High-spectral-resolution stimulated Rayleigh–Brillouin scattering at 1 μm," Opt. Lett. **26**, 1894-1896 (2001).

C. Jirauschek, E. M. Jeffrey, and G. W. Faris, "Electrostrictive and thermal stimulated Rayleigh spectroscopy in liquids," Phys. Rev. Lett. **87**, 233902 (2001).

K. S. Kalogerakis, B. Blehm, R. Forman, C. Jirauschek, and G. W. Faris, "Stimulated Rayleigh and Brillouin scattering in supercritical fluids," manuscript in preparation.

INTERACTIONS/TRANSITIONS

PRESENTATIONS

The following presentations were made on research supported by this contract:

C. Jirauschek, E. M. Jeffrey, G. W. Faris, "Stimulated electrostrictive and thermal Rayleigh scattering in liquids," Paper QMI5, presented at the Conference of Lasers and Electro-Optics / Quantum Electronics and Laser Science Conference (CLEO/QELS), Baltimore, Maryland, 8-10 May 2001.

G. W. Faris, M. Gerken, C. Jirauschek, D. Hogan, and Y. Chen, "High spectral resolution infrared stimulated Rayleigh/Brillouin scattering in liquids," Paper CtuZ5, presented at the Conference of Lasers and Electro-Optics / Quantum Electronics and Laser Science Conference (CLEO/QELS), Baltimore, Maryland, 8-10 May 2001.

G. W. Faris, K. S. Kalogerakis, B. Blehm, R. Forman, and C. Jirauschek, "Stimulated Rayleigh and Brillouin scattering in supercritical fluids," presented at the Western spectroscopy Association Conference Asilomar Conference Center, Pacific Grove, CA30 January - 1 February 2002

INTERACTIONS

The following interactions occurred at the AFOSR/ARO contractors meeting in Chemical Propulsion, University of Southern California, 18-19 June, 2001:

Tim Edwards, supercritical fuels, diagnostic requirements, and supercritical cells.

Judy Wornat, supercritical diagnostics.

Jim Gord, laser diagnostics.

Mel Roquemore, miscellaneous research on combustion and fuels.

Tom Jackson, high pressure and hypersonic diagnostics.

Med Colket, combustion.

Paul Dimotakis, vortices in supersonic free jets.

Fred Gouldin, diagnostics.

Stephen Pope, combustion.

Ed Law, combustion chemistry.

Ron Hansen, laser diagnostics.

Fred Schauer, pulse detonation propulsion.

Galen King, diagnostics.

Other interactions:

Robert Boyd, University of Rochester, stimulated Rayleigh scattering.

Roger Hermann, Pennsylvania State University, stimulated Rayleigh scattering.

TRANSITIONS

None.

INVENTIONS

None.

HONORS/AWARDS

Gregory Faris, ARCS Fellow, 1985-1986

Associate editor, *Applied Optics*

APPENDIX A

HIGH-SPECTRAL-RESOLUTION STIMULATED RAYLEIGH–BRILLOUIN SCATTERING AT 1 μM, OPT. LETT. 26, 1894-1896 (2001).

High-spectral-resolution stimulated Rayleigh–Brillouin scattering at 1 μm

Gregory W. Faris, Martina Gerken, Christian Jirauschek, DaNel Hogan, and Yihong Chen

Molecular Physics Laboratory, SRI International, 333 Ravenswood Avenue, Menlo Park, California 94025-3493

Received August 23, 2001

We have demonstrated stimulated Rayleigh–Brillouin scattering at a wavelength of 1.064 μm, using an injection-seeded Nd:YAG laser as a pump laser and a tunable diode laser as a probe laser. Spectra with a good signal-to-noise ratio are obtained despite the low probe-beam power and small gain coefficient in the infrared. Stimulated Rayleigh scattering is readily observable in organic and many other liquids because of absorption by the OH and CH overtone or combination bands. The absorption also causes an asymmetry in the stimulated Brillouin peak. A Rayleigh linewidth of 8 MHz is measured with this approach. © 2001 Optical Society of America

OCIS codes: 290.5900, 300.6320, 190.1900, 300.6340.

Stimulated scattering may be used to perform noninvasive *in situ* measurements of material physical properties. Stimulated Rayleigh and stimulated Brillouin scattering provide information on the thermal and elastic properties, respectively, of the material under study. Linewidths for stimulated Rayleigh and stimulated Brillouin scattering are typically of the order of 10 and 100 MHz, respectively, requiring narrow-band lasers for measurement.

These measurements are nonresonant and may be performed at any wavelength for which the medium under study is transparent or nearly transparent. Previous experiments on high-resolution stimulated Rayleigh and Brillouin scattering have used a ring dye laser as either a pump or a probe laser.[1–3] As an alternative to ring dye lasers, we use an external cavity laser diode operating at 1.064 μm. Although this laser provides more than an order of magnitude less power than a ring dye laser and the gain coefficient is more than four times smaller at 1.064 μm than at 532 nm,[4] we obtain spectra with good signal-to-noise ratios. In addition, stimulated Rayleigh peaks are readily observable.

At 1.064 μm, organic and many other liquids have optical absorption that is due to overtone or combination bands of OH or CH stretch vibrations. As shown below, this absorption causes significant changes in the stimulated Rayleigh and stimulated Brillouin spectra compared with measurements performed in the visible spectral region, where many liquids have little or no absorption.

Brillouin and Rayleigh scattering occur as a result of refractive-index fluctuations caused by acoustic waves and nonpropagating entropy (thermal) fluctuations, respectively. At high light intensities, stimulated Brillouin and Rayleigh scattering can occur, wherein growth occurs for both the scattered wave and the material fluctuation. For stimulated Rayleigh and Brillouin scattering, there are two primary mechanisms for coupling the electric field of the light and the material fluctuations—electrostriction and absorption.[5] The electrostrictive effect (the change in density produced by a spatially varying electric field through the linear polarizability of the medium) produces stimulated scattering in the absence of absorption. When there is optical absorption, thermal expansion also causes material fluctuations. For pure electrostrictive scattering, stimulated Rayleigh scattering is typically of the order of 100 times smaller than stimulated Brillouin scattering and is extremely difficult to observe. However, with absorption, the stimulated thermal Rayleigh scattering can become larger and easily observed.

Our experimental apparatus for stimulated scattering at 1.064 μm is shown in Fig. 1. The pump laser is an injection-seeded Nd:YAG laser. This laser provides the high peak powers necessary for stimulated scattering measurements and the narrow linewidths required for resolution of the narrow spectral features. By reduction of the oscillator pump energy, Fourier-transform-limited spectral linewidths as narrow as 20 MHz have been obtained with this laser at 532 nm.[6] The probe laser is a diode laser, tuned through feedback from an external grating (Environmental Optical Sensors Model 2010). The laser cavity is thermally stabilized, but no active frequency stabilization has been applied. The elongated beam profile of the diode laser is reduced and circularized with an anamorphic prism pair (Melles Griot 06 GPA 003), producing a beam of roughly 1 mm in diameter. An acousto-optic modulator directs the probe beam to a Fizeau wavelength meter (New Focus

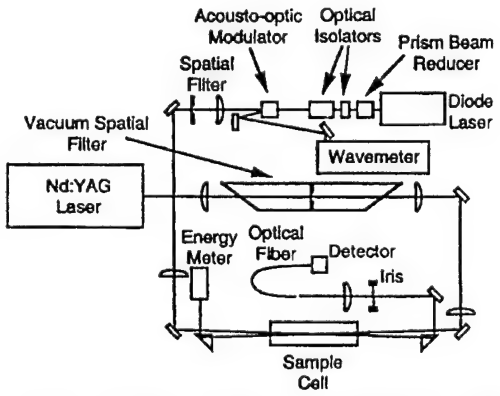

Fig. 1. Experimental apparatus for stimulated Brillouin and stimulated Rayleigh scattering at 1.064 μm.

0146-9592/01/231894-03$15.00/0

Model 7711), except for a 15-ms window centered at the time of the pump pulse, when the modulator is turned off and the probe beam passes to the sample. Spatially filtering both the pump and probe beams removes the higher-order transverse mode structure. The pump and probe beams overlap in a cell containing the liquid in a counterpropagating geometry with a crossing angle of approximately 25 mrad. The gain signal is detected with a InGaAs photodiode (Fermionics FD100FC) and a transimpedance amplifier. To provide spectra that are linear in the gain coefficient we use stimulated signals of approximately 1% of the probe beam. To avoid transient effects we measure the time-integrated gain signal.[4]

For a typical measurement we use a pulse energy of ~50 μJ, which corresponds to approximately 10^6 times more power than the diode laser. To prevent scattered Nd:YAG light from influencing the diode laser we use two optical isolators on the diode laser beam. We prevent scattered pump-laser light from overwhelming the gain signal by spatially filtering the detected light with an iris, a lens, and a 62.5-μm-core optical fiber coupled to the InGaAs photodiode.

We use two methods to determine the relative wavelength of the diode laser: (1) direct measurement with a wavemeter and (2) the heterodyne frequency obtained by means of mixing the diode laser and seed laser beams on a detector and measured with a digital oscilloscope. Comparison of 16 measurements with the two methods agreed to within 1.5%.

A stimulated Rayleigh–Brillouin spectrum for *n*-hexane obtained with this system is shown as the top curve in Fig. 2. The abscissa is the difference in frequency between the probe and pump lasers determined by the wavemeter. We divide the gain signal by the pump- and probe-laser intensities to compensate for intensity fluctuations in each laser. The outer two peaks are Brillouin peaks; the central pair of peaks is due to stimulated thermal Rayleigh scattering. The positive Brillouin peak to the left is a gain peak, corresponding to transfer of power from the Nd:YAG laser to the probe laser. The negative peak to the right is a loss peak, wherein power is transferred from the probe laser to the pump laser.

We performed fits to the measured line shapes to determine linewidths, line shifts, and peak heights. The electrostrictive Brillouin line shape is described by the real (absorptive or symmetric) part of a complex Lorentzian profile; the thermal Brillouin and Rayleigh line shapes are described by the imaginary (dispersive or asymmetric) parts of a complex Lorentzian profile.[5] The measured line shapes are given by the convolution of the Gaussian spectral line shape of the Nd:YAG pump laser with these Lorentzian profiles. These convolved line shapes may be expressed as the real and imaginary parts of the complex error functions of the Brillouin and Rayleigh peaks, respectively (the former is a Voigt profile). Nonlinear least-squares fits to the data were performed with the Igor graphics program (WaveMetrics) and the complex error function algorithm of Humlicek.[7,8] We used the Fourier-transform-limited linewidth calculated from pulse width as the spectral linewidth of the pump laser. To eliminate the contribution of the 10-Hz dither used to lock the Nd:YAG laser to the seed laser we performed measurements at 5 Hz. The seed-laser linewidth is specified to be less than 300 kHz in 50 ms.

The full fit to the Rayleigh–Brillouin spectrum is shown as the curve labeled Fit in Fig. 2. Very good agreement is found between the measured and fitted line shapes (see also Figs. 3 and 4). The electrostrictive and thermal contributions to the overall fit are shown separately at the bottom of Fig. 2. The dispersive Lorentzian shape of the thermal Brillouin scattering creates an asymmetry for the Brillouin peaks. This can be seen more clearly from Fig. 3, which shows the Brillouin gain peak from Fig. 2.

A scan over the stimulated Rayleigh peak is shown in Fig. 4. The frequency values were determined from the heterodyne signal. This peak is quite narrow. The average linewidth determined from multiple fits such as those shown in Fig. 4 is 8.5 ± 3.1 MHz, which is in agreement with the value expected from the thermal diffusivity for *n*-hexane. These measurements were performed with a pulse width of the Nd:YAG laser of approximately 30 ns, which corresponds to a a FWHM spectral linewidth of ~15 MHz.

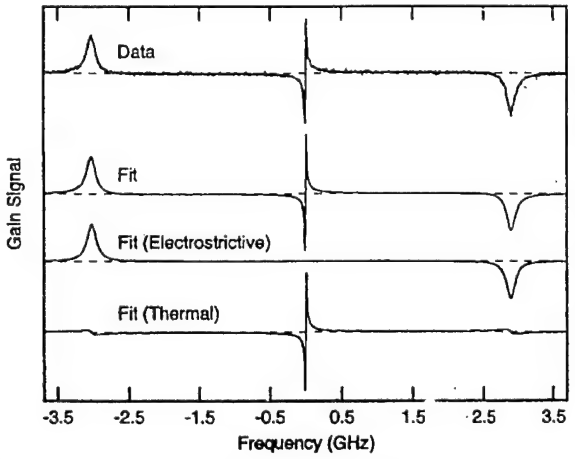

Fig. 2. Stimulated Rayleigh–Brillouin spectrum for *n*-hexane at 1.064 μm (top curve), fits to the data (middle curves), and electrostrictive and thermal components of the fit (bottom curve). The dashed lines indicate the zero gain level for each curve.

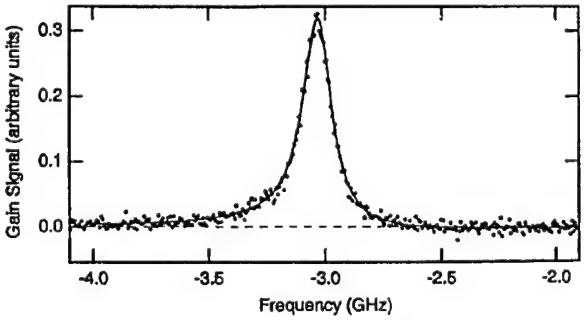

Fig. 3. Data (points) and fit (solid curve) for stimulated Brillouin gain peak for *n*-hexane at 1.064 μm. Stimulated thermal Brillouin scattering gives an asymmetry to the peak.

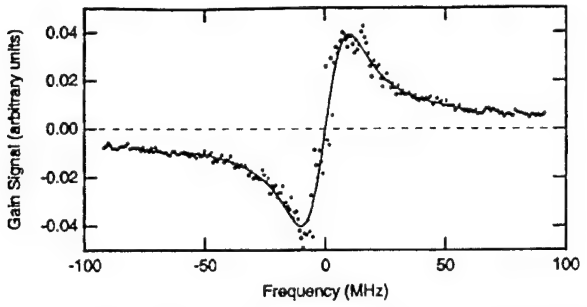

Fig. 4. Data (points) and fit (solid curve) for stimulated thermal Rayleigh scattering in n-hexane at 1.064 μm.

Table 1. Properties Measured in Hexane by Stimulated Rayleigh–Brillouin Scattering at 1.064 μm

Property	Our Results	Literature Value
Brillouin shift (GHz)	2.92 ± 0.06	
Brillouin width (MHz)	148 ± 7	
Rayleigh width (MHz)	8.5 ± 3.1, 7.9 ± 3.6	6.6[a]
γ_e/γ_a	8.4 ± 0.7 8.0 ± 0.9	~6[a,b]
Acoustic Lifetime (ns)	1.08	
Acoustic velocity (km/s)	1.15	1.11[c]
Thermal diffusivity (m^2/s)	1.0×10^{-7}	8.1×10^{-8} [a]

[a]Calculated from theory[5] by use of literature parameter values.[10]

[b]Calculated with $\gamma_e \approx (n^2 - 1)(n^2 + 2)/3$ and our measured absorption coefficient for hexane at 1.064 μm (0.05 cm^{-1}).

[c]Ref. 11.

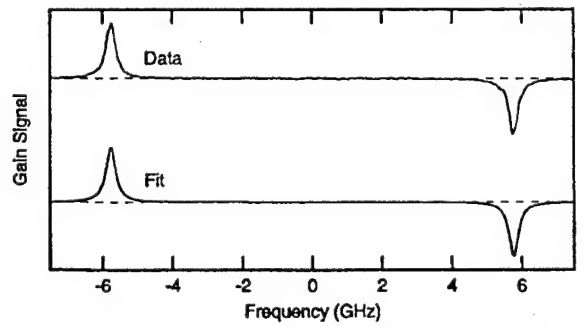

Fig. 5. Stimulated Brillouin spectrum for methanol measured at 532 nm.

Thus the laser linewidth is approximately twice the measured linewidth of the Rayleigh peak. The good agreement between the measured and calculated Rayleigh linewidths confirms that the Nd:YAG laser has a transform-limited linewidth of 15 MHz. The second Rayleigh linewidth in Table 1 is calculated from the Brillouin width, thermal Brillouin height, and Rayleigh height[5] and agrees with the directly measured linewidth.

The spectroscopic and thermodynamic properties of n-hexane, determined from spectroscopic fits, are given in Table 1. The errors are standard deviations of values averaged from 14 or more measurements. We use the refractive index, n, of hexane (1.357, extrapolated to 1.064 μm from an expression in Ref. 9) to determine the acoustic velocity and the thermal diffusivity.[5] The values of the ratio of the electrostrictive and absorptive coupling coefficients, γ_e/γ_a, are determined by comparison of the electrostrictive Brillouin peak with the absorptive Rayleigh and absorptive Brillouin peaks (first and second values, respectively, in Table 1). The agreement of these two measured values confirms the theoretical relationship[5] between these peaks. Good agreement is obtained between our measurements and values available in the literature.

For comparison, a stimulated scattering spectrum of methanol taken at 532 nm is shown in Fig. 5. This spectrum was acquired by use of the second harmonic of the same Nd:YAG laser and a cw ring dye laser (Coherent CR-699) as a probe laser. The spectra taken at 1.064 μm (Fig. 2) and 532 nm (Fig. 5) are of similar quality, except that the infrared measurement has a strong stimulated thermal Rayleigh peak.

The ability to perform stimulated scattering in the infrared offers unique possibilities for materials that are only transparent in the infrared. Measurements of spontaneous Brillouin or Rayleigh scattering in the infrared are greatly hampered by small scattering cross sections and poor detector performance. However, with stimulated scattering the signal powers can be nearly as large as the laser power, overcoming these limitations. This approach allows bulk measurement in materials, such as most semiconductors and liquids containing multiring aromatic compounds, that are not transparent in the visible.

This work was supported by the U.S. Air Force Office of Scientific Research under contracts F49620-97-C-0002 and F49620-01-C-0020. D. Hogan was supported by the Research Experiences for Undergraduates program of the National Science Foundation.

References

1. S. Y. Tang, C. Y. She, and S. A. Lee, Opt. Lett. **12,** 870–872 (1987).
2. G. W. Faris, L. E. Jusinski, M. J. Dyer, W. K. Bischel, and A. P. Hickman, Opt. Lett. **15,** 703–705 (1990).
3. K. Ratanaphruks, W. T. Grubbs, and R. A. MacPhail, Chem. Phys. Lett. **182,** 371–378 (1991).
4. G. W. Faris, L. E. Jusinski, and A. P. Hickman, J. Opt. Soc. Am. B **10,** 587–599 (1993).
5. W. Kaiser and M. Maier, in *Laser Handbook*, F. T. Arecchi and E. O. Schulz-Dubois, eds. (North-Holland, Amsterdam, 1972), Vol. 2, pp. 1077–1150.
6. G. W. Faris, M. J. Dyer, and W. K. Bischel, Opt. Lett. **19,** 1529–1531 (1994).
7. J. Humlicek, J. Quant. Spectrosc. Radiat. Transfer **27,** 437–444 (1982).
8. F. Schreier, J. Quant. Spectrosc. Radiat. Transfer **48,** 743–762 (1992).
9. H. El-Kashef, J. Mod. Opt. **46,** 1389–1399 (1999).
10. D. R. Lide, ed., *CRC Handbook of Chemistry and Physics*, 81st ed. (CRC, Boca Raton, Fla., 2000), pp. 6–137, 6–188, and 15–16.
11. H. Z. Cummins and R. W. Gammon, J. Chem. Phys. **44,** 2785–2796 (1966).

APPENDIX B

ELECTROSTRICTIVE AND THERMAL STIMULATED RAYLEIGH SPECTROSCOPY IN LIQUIDS, PHYS. REV. LETT. 87, 233902 (2001)

Electrostrictive and Thermal Stimulated Rayleigh Spectroscopy in Liquids

Christian Jirauschek, Elizabeth M. Jeffrey, and Gregory W. Faris
Molecular Physics Laboratory, SRI International, 333 Ravenswood Avenue, Menlo Park, California 94025–3493
(Received 22 June 2001; published 15 November 2001)

We have observed the spectrum of electrostrictive stimulated Rayleigh scattering in a liquid and created a transition to stimulated thermal Rayleigh scattering with the addition of an absorbing liquid. With the proper amount of absorption, the electrostrictive and thermal contributions to the scattering exactly cancel, resulting in no stimulated Rayleigh scattering. An absorption coefficient of 0.000 12 cm^{-1} is sufficient to cancel the electrostrictive Rayleigh scattering in Freon 113.

DOI: 10.1103/PhysRevLett.87.233902 PACS numbers: 42.65.Es, 33.20.Fb, 39.30.+w, 42.50.Vk

Rayleigh scattering involves the scattering of light by nonpropagating entropy or thermal fluctuations. These fluctuations produce spatial variations in refractive index and hence light scattering. When the incident light is sufficiently intense, stimulated Rayleigh scattering occurs.

In this Letter we describe the use of tunable Rayleigh gain spectroscopy in electrostrictive and predominantly absorptive liquids. We show that electrostrictive and thermal effects can cancel each other, resulting in no stimulated Rayleigh scattering, in agreement with theory [see Eq. (1) below] [1]. Complete cancellation of a stimulated scattering process has not been observed previously to our knowledge. Cancellation of stimulated Raman scattering due to Stokes/anti-Stokes coupling has been observed [2], but this cancellation occurs only at a specific phase-matching angle. The combination of electrostrictive and absorptive effects leads to the reduction of the stimulated Brillouin gain over a part of the spectral profile [3], but with a proportional increase in gain over a different portion of the spectral profile.

Two primary mechanisms can produce the coupling between light and medium for stimulated Rayleigh scattering—electrostriction and light absorption. For stimulated electrostrictive Rayleigh scattering, the thermal fluctuations are produced indirectly as a result of the electrostrictive density fluctuations, and the process is relatively weak. In absorptive media, thermal fluctuations are produced directly by absorption of light, leading to much larger gains for stimulated thermal Rayleigh scattering. A third mechanism, the electrocaloric effect, can cause stimulated Rayleigh scattering through direct coupling of the electric field and temperature. This effect is negligible in most circumstances [4].

Stimulated electrostrictive Rayleigh scattering is much more difficult to observe than stimulated thermal Rayleigh scattering [5,6] and stimulated Rayleigh wing scattering [7,8] (scattering by fluctuations in the orientation of anisotropic molecules). Early experiments in gases [9] and liquids [10,11] resulted in spectrally shifted scattered light that was attributed to pure stimulated Rayleigh scattering. Later work using gain spectroscopy resulted in partially resolved peaks from electrostrictive stimulated Rayleigh scattering in a gas [12]. We measured the stimulated Rayleigh peak in a liquid using stimulated gain spectroscopy. The Rayleigh peak is spectrally resolved and isolated from the stimulated Brillouin peak, allowing confirmation that the electrostrictive stimulated Rayleigh scattering matches the anticipated line shape.

In gain spectroscopy, the amplification or gain of the scattered light produced by a strong pump light beam is monitored using a second probe light beam. The spectral variation in gain for the probe beam is given by the imaginary part of a complex Lorentzian function [1]:

$$g_{\mathrm{RL}} = [g^{a}_{\mathrm{RL}}(\max) - g^{e}_{\mathrm{RL}}(\max)]\frac{4\nu/\Delta\nu_{\mathrm{RL}}}{1 + (2\nu/\Delta\nu_{\mathrm{RL}})^2}, \tag{1}$$

where $\Delta\nu_{\mathrm{RL}}$ is the spontaneous Rayleigh linewidth, $g^{e}_{\mathrm{RL}}(\max)$ and $g^{a}_{\mathrm{RL}}(\max)$ are the maximum values for the electrostrictive and the absorptive gain factors, respectively, and $\nu = \nu_s - \nu_p$ is the difference between the frequencies ν_s of the probe (or scattered) beam and ν_p of the pump beam.

The experimental apparatus used to measure the frequency dependence of the gain factor is illustrated in Fig. 1. Ray trajectories are represented by dotted lines. We use the light from an injection-seeded, homebuilt, single-mode Nd:YAG laser [13] at 1064 nm to provide the pump radiation. We operate this laser at 10 Hz with a full width at half maximum pulse duration of about 29 ns, which results in a Fourier transform limited spectral bandwidth of about 15 MHz. The probe light is provided by a tunable single-mode diode laser (Environmental Optical Sensors, Inc., model 2010) with a linewidth smaller than 300 kHz in 50 ms.

The spatial filters serve to suppress higher order transverse spatial modes. Furthermore, the spatial filter in the probe beam trajectory, together with the two optical isolators, prevents pump light from reaching the resonator of the tunable laser, which would otherwise cause frequency and amplitude fluctuations on the probe beam. Inside the cell, the counterpropagating (~180° crossing angle) pump and probe beams are overlapped at their focal points to obtain an optimal gain signal. The beam spot sizes at the focus are approximately 385 and 260 μm ($1/e^2$ beam radius) for the pump and probe beams, respectively.

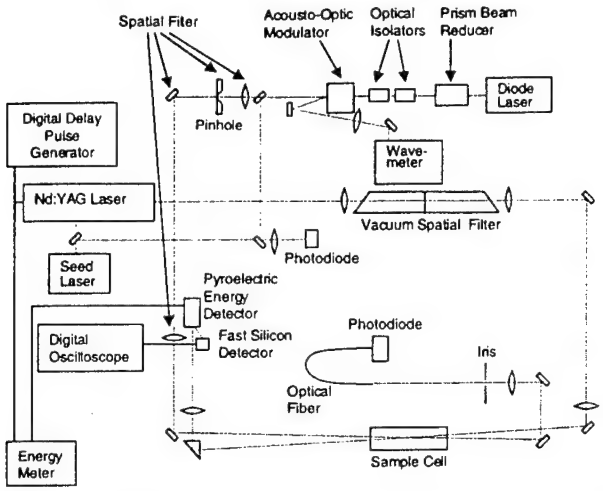

FIG. 1. Experimental apparatus for stimulated Rayleigh gain spectroscopy in liquids.

Detection is performed using an InGaAs photodiode with a transimpedance amplifier. The output signal is split with a bias tee into a high frequency portion, which is the gain signal for the ~29 ns pulse, and a low frequency part, which monitors the probe beam power. The energy of the Nd:YAG beam is measured with a pyroelectric energy detector. The measured gain signals are divided by the probe and pump beam powers to compensate for fluctuations in the laser powers. A fast silicon detector is used to measure the pulse duration of the pump beam. Portions of the seed laser and probe laser are mixed on a second InGaAs photodiode to directly measure the relative frequency between the two lasers for measurements on the Rayleigh peak. For Figs. 4 and 5 below, the probe wavelength was measured using a wave meter.

Because the time constants for Rayleigh scattering are typically longer than the laser pulse width, transient effects are important [14,15]. We eliminate these transient effects by measuring the time-integrated gain signal, a method that was used previously for stimulated Brillouin scattering [16]. Using the transient expressions for stimulated electrostrictive and thermal Rayleigh scattering [17] and following the analysis used for stimulated Brillouin scattering [16], is may be easily shown that the time-integrated gain signal spectrum provides a simple measurement of the convolution of the laser and Rayleigh line shapes.

We used Freon 113 (1,1,2-trichlorotrifluoroethane from Aldrich Chemical Co., 99.8%, <0.005% water) to observe stimulated electrostrictive Rayleigh scattering because it does not absorb light at 1064 nm. Most liquids containing hydrogen atoms have optical absorption at 1064 nm due to overtone or combination vibrational bands.

We used pump beam energies of about 5 mJ in a 30 ns pulse to observe the pure electrostrictive signal in Freon 113. This corresponds to a power of about 10^8 times larger than the ~1 mW of probe beam power available at the sample cell. To enable measurement of spectra linear in the gain coefficient, the gain signals were approximately 1% of the probe beam power. Thus even a small fraction of scattered pump light can completely overwhelm the electrostrictive gain signal. This effect is exacerbated by the fact that the pump and probe beams have nearly identical frequencies in the region of the Rayleigh peak. Thus, a heterodyne signal between the probe beam and scattered pump light is also present at the detector used to measure the gain signal. This heterodyne process provides an effective amplification of the scattered pump light since the detected heterodyne signal is proportional to the square root of the product of the pump and probe powers. Thus the 1% gain signal is only as big as the heterodyne signal from a scattered pump light power of 10^{-4} of the probe beam power, or 10^{-12} of the pump beam power.

The influence of scattered pump light was reduced by using very clean windows and Freon, by tilting the sample cell to direct reflections from the windows away from the detector, blocking all stray reflections and other scattered light with black screens, making the pump and probe beams of approximately the same diameter, spatially filtering the pump and probe beams to remove higher order transverse spatial modes, and spatially filtering the probe beam before the detector using an iris, lens, and multimode fiber. However, we could not reduce the scattered light below the level produced by spontaneous Rayleigh scattering of the Freon in the volume determined by the overlap between the pump and probe beams. This spontaneous Rayleigh scattering is the dominant noise source for our measurements. We reduced the influence of the heterodyne signal from spontaneous Rayleigh scattering by averaging the measured gain over many laser shots (typically 60 shots for the stimulated Rayleigh measurements). Because the pump and probe beams are not phase locked, the heterodyne signal should average to zero. We could not use the Nd:YAG laser to amplify the probe beam before the liquid cell because that would limit the gain observation time sufficiently to introduce transient effects, which would distort the line shapes.

The solid curve at the top of Fig. 2 shows the measured electrostrictive Rayleigh gain signal in Freon 113. The width of the Rayleigh peak is broadened considerably by the spectral linewidth of the pulse laser. The dashed curve shows the result of fitting the line shape of Eq. (1), convolved with the Gaussian spectral profile of the pump laser. The linewidth of the Rayleigh peak, calculated [1] using known properties of the Freon [18], is 4 MHz. The linewidth of the pump laser was fixed at the Fourier transform limited width determined from the pulse duration (15 MHz). The contribution of the probe laser linewidth is negligible. Measurements were performed at a 5 Hz repetition rate to eliminate contributions of the 10 Hz frequency dither used to lock the Nd:YAG laser to the seed laser. The fit is good considering the only free parameter is the peak height.

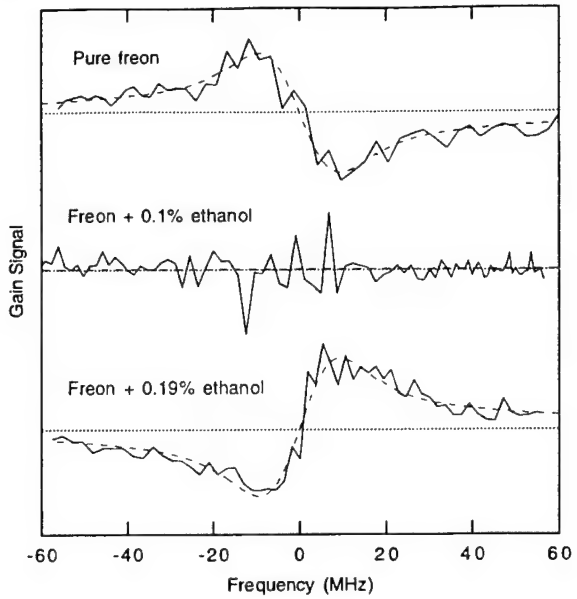

FIG. 2. Measured stimulated Rayleigh gain signal (solid curves) and fitted profile (dashed curves) in pure Freon 113 (top), Freon with 0.1% ethanol (middle), and Freon with 0.19% ethanol (bottom) as a function of the frequency difference between the probe and pump lasers.

To produce some absorption in the Freon, we used ethanol, which mixes with Freon and has moderate absorption at 1064 nm. The Freon and ethanol both comprise a pair of single-bonded carbon atoms, but differ in the atoms surrounding the carbons. After adding 0.10% (volume percentage) of ethanol, the electrostrictive and absorptive gains have the same value and cancel each other out [see Eq. (1)]. The curve measured for this condition is shown in the middle of Fig. 2. The Rayleigh gain signal (solid curve) shows no Rayleigh peak, and the curve fitting (dashed curve) produces a flat line. The small variations in the measured gain signal are due to the heterodyne signal from scattered pump light. After doubling the amount of ethanol in Freon 113, we obtain a gain signal that has about the same height as in pure Freon, but is inverted. The measured gain signal for 0.19% of ethanol is shown at the bottom of Fig. 2 (solid curve); the dashed curve is the fitted profile.

We measured the absorption coefficient for different volume percentages of ethanol in Freon. The absorption coefficient displays a linear dependence on the percentage of ethanol, rising from zero in pure Freon to 0.117 cm^{-1} for pure ethanol. This measurement shows that a very small absorption coefficient (0.000 12 cm^{-1}) is sufficient to cause the cancellation of the electrostrictive Rayleigh scattering at 0.1% ethanol.

For small amounts of ethanol in Freon the physical properties (apart from the absorption) are changed only little. Theory [1] predicts a linear growth of the maximum absorptive gain factor $g^a_{RL}(\max)$ with the absorption

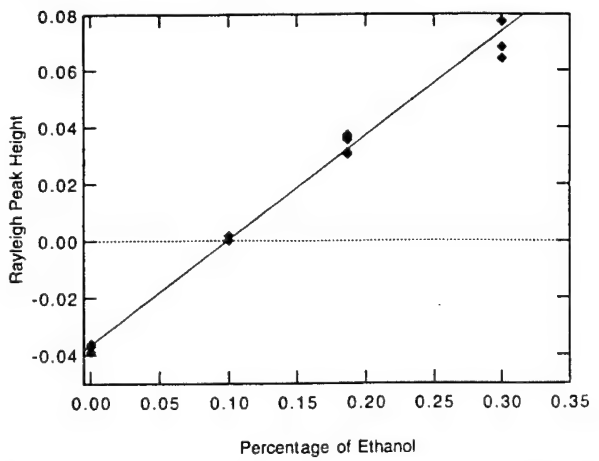

FIG. 3. Measured heights of the fitted Rayleigh peak in a mixture of Freon 113 and ethanol.

coefficient, whereas the maximum electrostrictive gain factor $g^e_{RL}(\max)$ does not depend on the absorption. Measurements of the gain signal were performed for various amounts of ethanol in Freon, and the height of the Rayleigh peak was determined from fits as in Fig. 2. The results are shown in Fig. 3 for small percentages of ethanol. We display peak height rather than peak area as the area of the Rayleigh peak is infinite [Eq. (1) behaves as $1/\nu$ for large ν]. As expected, the height displays a linear dependence on the absorption coefficient [or $g^e_{RL}(\max) - g^a_{RL}(\max)$]. The height has a negative value for $g^a_{RL}(\max) = 0$ in pure Freon, becomes zero for $g^a_{RL}(\max) = g^e_{RL}(\max)$, corresponding to 0.1% of ethanol, and has positive values for $g^a_{RL}(\max) > g^e_{RL}(\max)$.

When the probe laser is scanned over a larger frequency range, stimulated Brillouin scattering is observed. The

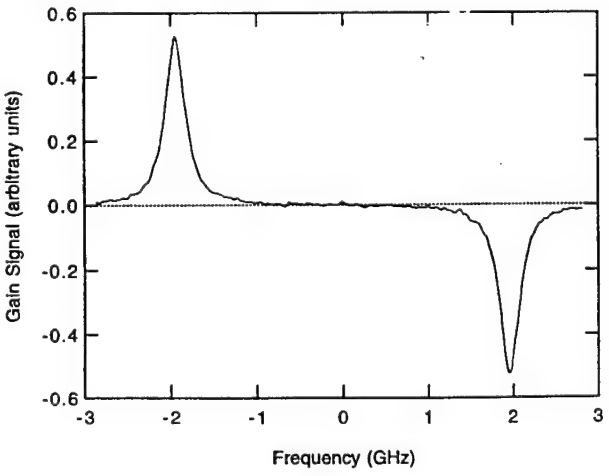

FIG. 4. Measured stimulated Brillouin gain signal in pure Freon 113 as a function of the frequency difference between the probe and pump lasers. The stimulated Rayleigh gain signal of Fig. 2 is too small to be seen in this figure.

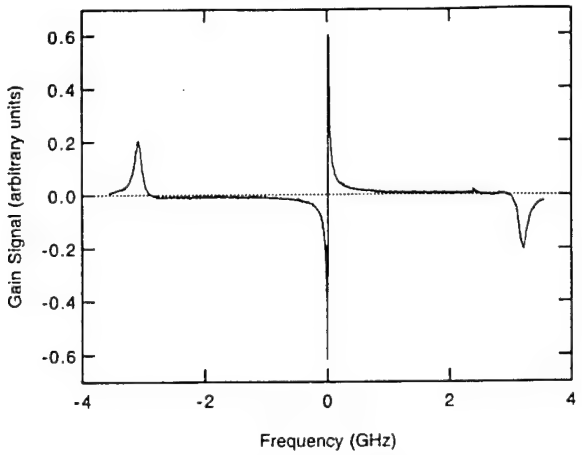

FIG. 5. Measured stimulated Brillouin gain signal in ethanol as a function of the frequency difference between the probe and pump lasers. Absorption produces a large stimulated thermal Rayleigh peak and stimulated thermal Brillouin scattering, which causes asymmetry of the stimulated Brillouin peaks.

shapes of the stimulated electrostrictive and thermal Brillouin scattering peaks are described by the real and imaginary parts of the complex Lorentzian profile, respectively [1]. Only stimulated electrostrictive Brillouin scattering is observed in pure Freon 113 (Fig. 4). Gain and loss peaks are observed at the left and right of Fig. 4, respectively. The gain and loss peaks correspond to the transfer of energy from the pump laser to the probe laser and vice versa. The stimulated electrostrictive Rayleigh scattering, which is typically about 100 times smaller than the stimulated electrostrictive Brillouin scattering, is too small to be seen in Fig. 4.

The modest absorption coefficient of ethanol at 1064 nm ($0.12\ \mathrm{cm}^{-1}$) is sufficient to cause very large stimulated thermal Rayleigh scattering in ethanol, which is now much larger than the stimulated Brillouin scattering peak (Fig. 5). Stimulated thermal Brillouin scattering, which, like the Rayleigh peak, is described by the imaginary part of the complex Lorentzian, causes asymmetry of the Brillouin peaks in ethanol.

We reported an experimental investigation of stimulated Rayleigh scattering in liquids by tunable Rayleigh gain spectroscopy. We observed the electrostrictive Rayleigh peak in a liquid (Freon 113). By adding small amounts of ethanol, we increased the absorption coefficient to the point where electrostrictive and absorptive gain cancel. For a further increase of the absorption, the peak inverts from its original form. In agreement with theory, a linear relationship between the height of the peak and the absorption coefficient was observed.

This work was supported by the Air Force Office of Scientific Research under Contracts No. F49620-97-C-0002 and No. F49620-01-C-0020. E. M. J. was supported by the Research Experiences for Undergraduates Program of the National Science Foundation.

[1] W. Kaiser and M. Maier, in *Laser Handbook,* edited by F. T. Arecchi and E. O. Schulz-Dubois (North-Holland, Amsterdam, 1972), Vol. 2, pp. 1077–1150.
[2] M. D. Duncan, R. Mahon, R. Reintjes, and L. L. Tankersley, Opt. Lett. **11**, 803–805 (1986).
[3] D. Pohl, I. Reinhold, and W. Kaiser, Phys. Rev. Lett. **20**, 1141–1143 (1968).
[4] K. H. Wang and R. M. Herman, Phys. Rev. A **7**, 1248–1251 (1973).
[5] R. M. Herman and M. A. Gray, Phys. Rev. Lett. **19**, 824–828 (1967).
[6] D. H. Rank, C. W. Cho, N. D. Foltz, and T. A. Wiggins, Phys. Rev. Lett. **19**, 828–830 (1967).
[7] D. I. Mash, V. V. Morozov, V. S. Starunov, and I. L. Fabelinskii, JETP Lett. **2**, 25–27 (1965).
[8] C. W. Cho, N. D. Foltz, D. H. Rank, and T. A. Wiggins, Phys. Rev. Lett. **18**, 107–109 (1967).
[9] I. L. Fabelinskii, D. I. Mash, V. V. Morozov, and V. S. Starunov, Phys. Lett. **27A**, 253–254 (1968).
[10] G. I. Zaitsev, Y. I. Kyzylasov, V. S. Starunov, and I. L. Fabelinskii, JETP Lett. **6**, 255–257 (1967).
[11] Y. P. Kyzylasov, V. S. Starunov, and I. L. Fabelinskii, JETP Lett. **11**, 66–69 (1970). The authors note a shift from slightly Stokes to slightly anti-Stokes shifted stimulated scattering when absorption is introduced.
[12] C. Y. She, G. C. Herring, H. Moosmüller, and S. A. Lee, Phys. Rev. Lett. **51**, 1648–1651 (1983).
[13] M. J. Dyer, W. K. Bischel, and D. G. Scerbak, Proc. SPIE Int. Soc. Opt. Eng. **912**, 32–36 (1988).
[14] W. Rother, D. Pohl, and W. Kaiser, Phys. Rev. Lett. **22**, 915–918 (1969).
[15] A. O. Creaser and R. M. Herman, Phys. Rev. Lett. **29**, 147–150 (1972).
[16] G. W. Faris, L. E. Jusinski, and A. P. Hickman, J. Opt. Soc. Am. B **10**, 587–599 (1993).
[17] W. Rother, Z. Naturforsch **25A**, 1120–1135 (1970).
[18] *CRC Handbook of Chemistry and Physics,* edited by Robert C. Weast (CRC Press, West Palm Beach, FL, 1978), 59th ed., pp. E34–E35.

APPENDIX C

STIMULATED RAYLEIGH AND BRILLOUIN SCATTERING IN SUPERCRITICAL FLUIDS, MANUSCRIPT IN PREPARATION

STIMULATED RAYLEIGH AND BRILLOUIN SCATTERING IN SUPERCRITICAL FLUIDS

Konstantinos S. Kalogerakis, Benjamin Blehm, Rachel Forman, Christian Jirauschek, and Gregory W. Faris
Molecular Physics Laboratory, SRI International
333 Ravenswood Avenue, Menlo Park, CA 94025-3493

ABSTRACT

We have performed stimulated Rayleigh / Brillouin scattering in n-hexane for a wide range of sub- and supercritical temperature and pressure conditions, including the near-critical region. Using 1064-nm light enhances stimulated Rayleigh scattering.

Supercritical fluids are important for a wide range of applications including chemical extraction and processing, processing waste, and high performance heat exchange systems. We show that stimulated Rayleigh and stimulated Brillouin scattering can be an effective tool for studying supercritical fluids. Rayleigh scattering and Brillouin scattering provide information on the thermal properties and elastic properties, respectively, of the material under study. These measurements may be performed at any wavelength for which the material is transparent. Stimulated Rayleigh / Brillouin measurements are generally performed in the visible wavelength region using a ring dye laser .[1-3] We have recently demonstrated that stimulated Rayleigh / Brillouin scattering may be performed quite well at a wavelength of 1.064 μm using a diode laser as a tunable probe laser.[4,5] An advantage of performing measurements at this wavelength is the strong enhancement of the stimulated Rayleigh scattering peak in most liquids produced through optical absorption at vibrational overtone or combination bands.

The optical arrangement for stimulated Rayleigh / Brillouin scattering is shown in Fig. 1. The pump laser is an injection seeded Nd:YAG laser. By lowering the oscillator pump energy, we obtain a transform-limited linewidth of about 10 MHz. The probe laser is an external cavity diode laser. The two lasers are overlapped in the cell in a counter-propagating geometry. To reduce scattered light, the measurement cell is tilted slightly and the probe light is spatially filtered through an optical fiber. The probe laser wavelength is measured using a Fizeau wavemeter. Because of the narrow linewidths of the Rayleigh peak, transient effects are important. We avoid transient effects by using the time-integrated gain signal.[4,6]

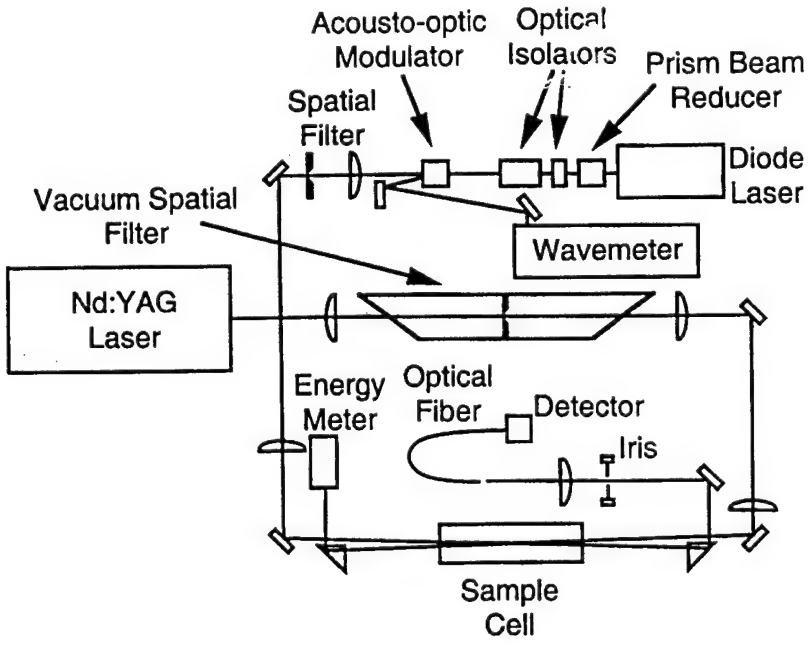

Fig. 1. Apparatus for stimulated Brillouin and stimulated Rayleigh scattering at 1064 nm.

The supercritical cell design is shown in Fig. 2. The cell comprises two windows separated by an internal length of 2.5 cm. The windows are sealed using graphite seals. Titanium bolts are used on the flanges holding the windows because titanium has nearly the same thermal expansion coefficient as the glass windows. The cell has been tested to temperatures as high as 600 °C and pressures as high as 14 MPa. A schematic of the overall high pressure system is shown in Fig. 3.

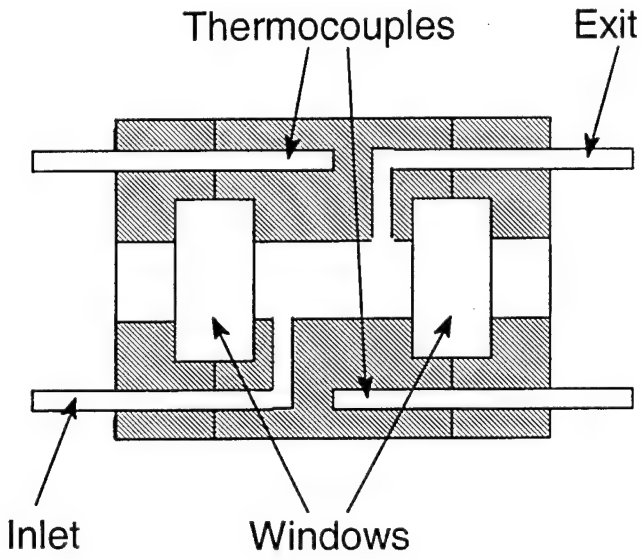

Fig. 2. Schematic diagram of the supercritical cell.

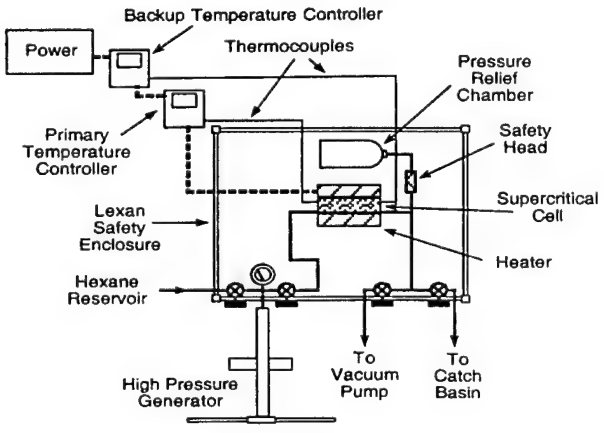

Fig. 3. Overall high pressure system.

Examples of stimulated Rayleigh / Brillouin scattering spectra measured in n-hexane near the critical temperature at three different pressures are shown in Fig. 4. The peaks to the left and right of each spectrum are the gain and loss Brillouin peaks, respectively. The central peak is the stimulated Rayleigh peak. Optical absorption has increased the size of the Rayleigh peak and produced asymmetry to the Brillouin peaks. Also shown in Fig. 4 are fits to the data (thicker lines). These fits include the appropriate lineshapes for each peak and the laser spectral width. Fits of this type enable calculation of material properties.

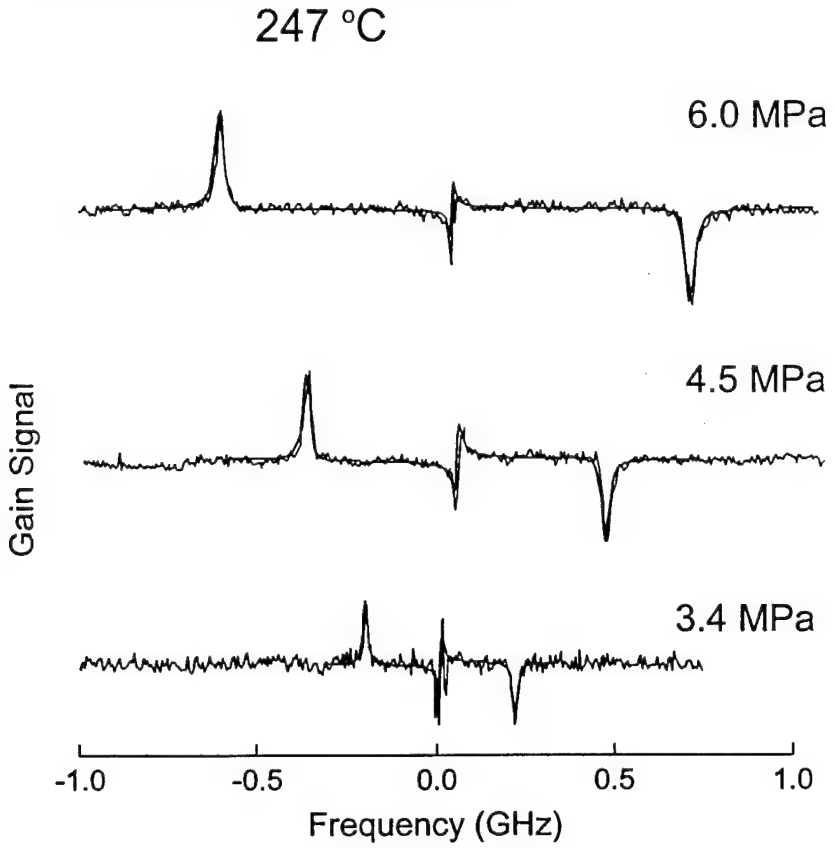

Fig. 4. Stimulated Rayleigh / Brillouin scattering spectrum for n-hexane measured at 1064 nm near the critical temperature for three different pressures. The spectral fits to the data including the electrostrictive and thermal components to the fit are shown.

The critical point for n-hexane occurs at a pressure 31 kPa and temperature of 234 ° C. Figures 5-9 present stimulated Brillouin scattering properties for n-hexane at 1064 nm at sub-, near-, and supercritical conditions. The striking feature in all the figures presented is the discontinuity in the observed properties that occurs at the critical point.

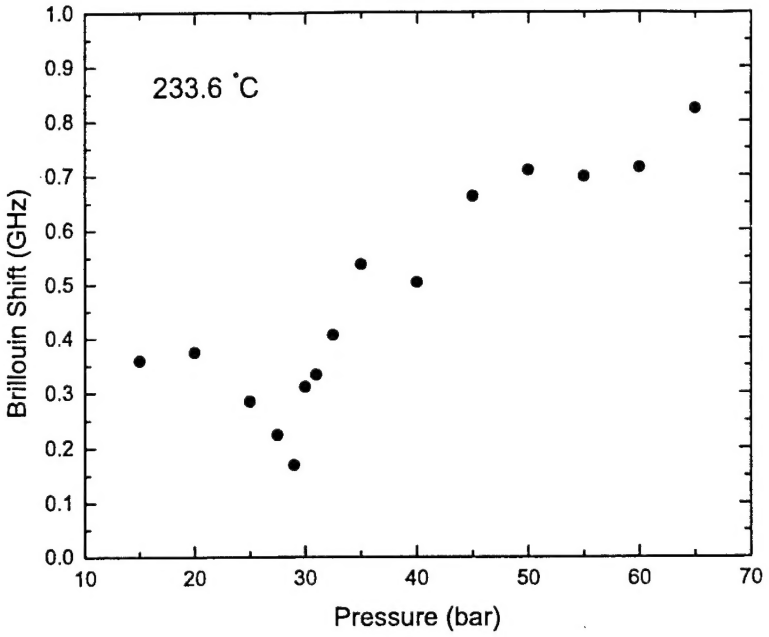

Fig. 5. The Brillouin shift observed in stimulated Brillouin scattering for n-hexane at 1064 nm near the critical temperature as a function of pressure. The Brillouin shift has a minimum in the region of the critical point.

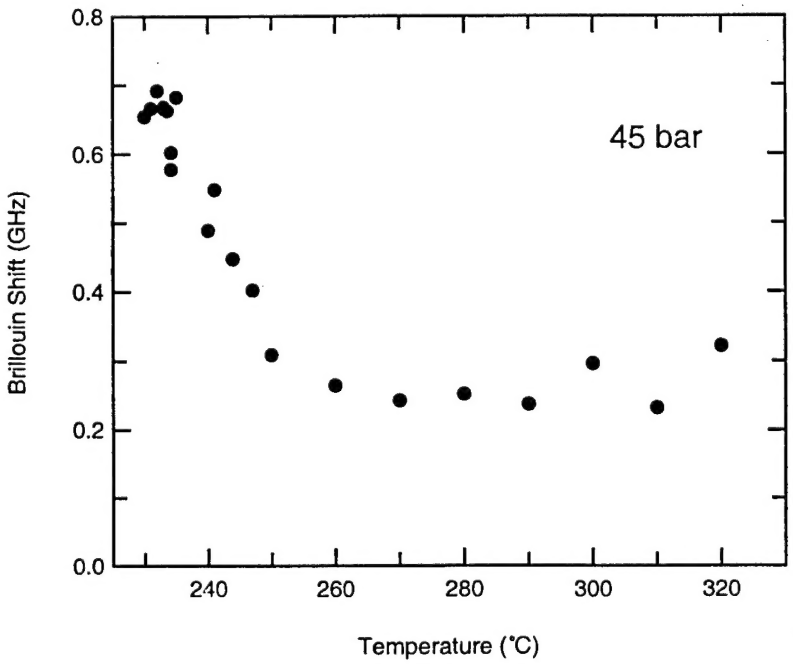

Fig. 6. The Brillouin shift observed in stimulated Brillouin scattering for n-hexane at 1064 nm for a pressure of 45 bar as a function of temperature. A local maximum is observed near the critical point.

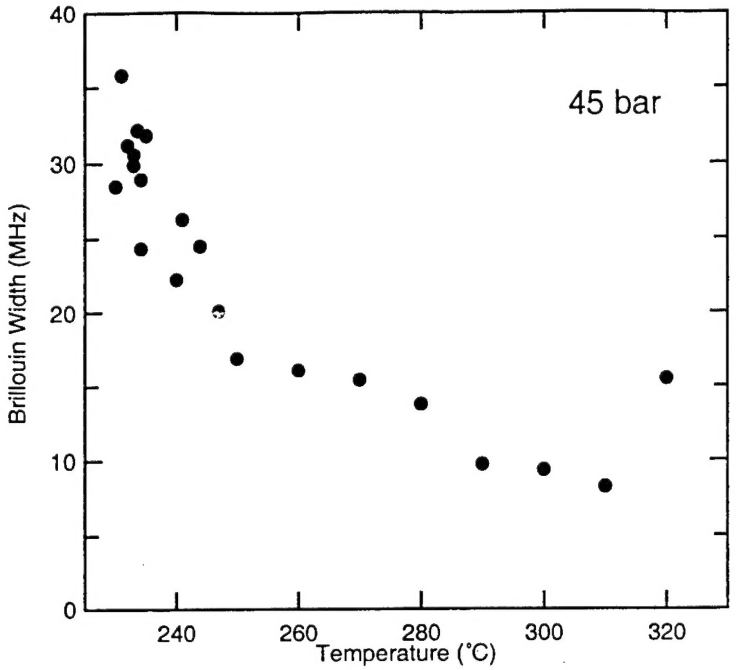

Fig. 7. The peak width observed in stimulated Brillouin scattering for n-hexane at 1064 nm for a pressure of 45 bar as a function of temperature.

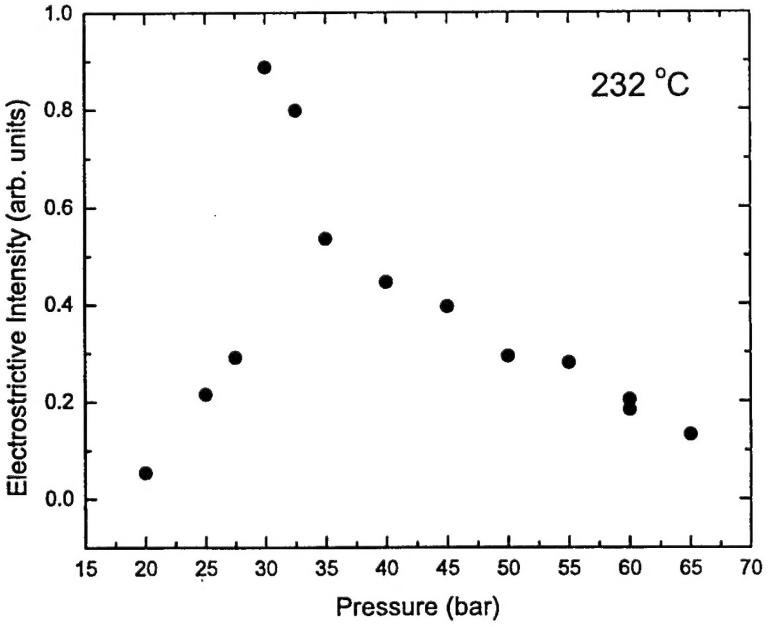

Fig. 8. The intensity of the electrostrictive component of stimulated Brillouin scattering for n-hexane at 1064 nm for a temperature of 232 ° C as a function of pressure. A sharp increase in intensity is observed near the critical point.

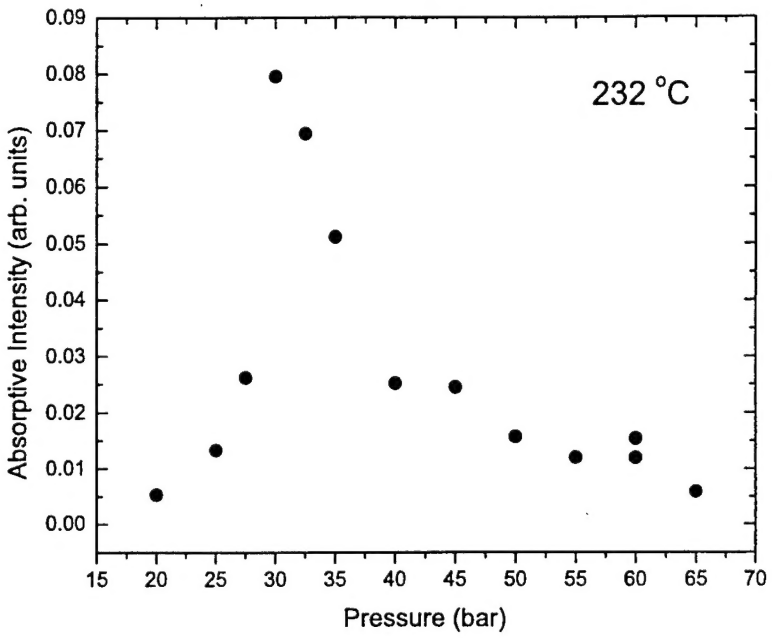

Fig. 9. The intensity of the absorptive component of stimulated Brillouin scattering for n-hexane at 1064 nm for a temperature of 232 ° C as a function of pressure.

ACKNOWLEDGMENTS

This work was supported by the Air Force Office of Scientific Research under contracts F49620-97-C-0002 and F49620-01-C-0020. R. Forman and B. Blehm were supported by the Research Experiences for Undergraduates program of the National Science Foundation.

REFERENCES

1. S. Y. Tang, C. Y. She, and S. A. Lee, "Continuous-wave Rayleigh-Brillouin-gain spectroscopy in SF_6," Opt. Lett. **12**, 870-872 (1987).

2. G. W. Faris, L. E. Jusinski, M. J. Dyer, W. K. Bischel, and A. P. Hickman, "High-resolution Brillouin gain spectroscopy in fused silica," Opt. Lett. **15**, 703-705 (1990).

3. K. Ratanaphruks, W. T. Grubbs, and R. A. MacPhail, "CW stimulated Brillouin gain spectroscopy of liquids," Chem. Phys. Lett. **182**, 371-378 (1991).

4. G. W. Faris, M. Gerken, C. Jirauschek, D. Hogan, and Y. Chen, "High-spectral-resolution stimulated Rayleigh–Brillouin scattering at 1 μm," Opt. Lett. **26**, 1894-1896 (2001).

5. C. Jirauschek, E. M. Jeffrey, and G. W. Faris, "Electrostrictive and thermal stimulated Rayleigh spectroscopy in liquids," Phys. Rev. Lett. **87**, 233902 (2001).

6. G. W. Faris, L. E. Jusinski, and A. P. Hickman, "High-resolution stimulated Brillouin gain spectroscopy in glasses and crystals," J. Opt. Soc. Am. B **10**, 587-599 (1993).